Revisiting Shadow Short-term Interest Rate Models: Evidence from the Ultra-Low
Interest Rate Environment in Japan

Hiroyuki Oi
Shigenori Shiratsuka
Shunichi Yoneyama

TCER

TOKYO CENTER FOR ECONOMIC RESEARCH
1-7-10-703 Iidabashi, Chiyoda-ku, Tokyo 102-0072, Japan

Abstract

Shadow short-term interest rate (SSR) models are expected to provide effective monetary policy indicators under the effective lower bound (ELB) constraint on nominal interest rates. This paper revisits the SSR models using yield curve data from the prolonged ultra-low interest rate environment in Japan. Specifically, this paper compares the various specifications of the SSR models based on the Nelson-Siegel model by focusing on a trade-off between estimation performance and theoretical consistency. This paper highlights the importance of evaluating monetary policy easing effects using the entire yield curve fluctuations, rather than relying solely on SSR estimates, especially in the ultra-low interest rate environment in Japan.

Hiroyuki Oi
Bank of Japan
Institute for Monetary and Economic Studies
2-1-1 Nihonbashi-Hongokucho, Chuo-ku, Tokyo, Japan
hiroyuki.ooi@boj.or.jp

Shigenori Shiratsuka
TCER
and
Keio University
Faculty of Economics
2-15-45 Mita, Minato-ku, Tokyo, Japan
shigenori.shiratsuka@keio.jp

Shunichi Yoneyama
Bank of Japan
Research and Statistics Department
2-1-1 Nihonbashi-Hongokucho, Chuo-ku, Tokyo, Japan
shunichi.yoneyama@boj.or.jp

Revisiting Shadow Short-term Interest Rate Models: Evidence from the Ultra-Low Interest Rate Environment in Japan [*]

Hiroyuki Oi,[†] Shigenori Shiratsuka,[‡] and Shunichi Yoneyama[§]

March 30, 2026

Abstract

Shadow short-term interest rate (SSR) models are expected to provide effective monetary policy indicators under the effective lower bound (ELB) constraint on nominal interest rates. This paper revisits the SSR models using yield curve data from the prolonged ultra-low interest rate environment in Japan. Specifically, this paper compares the various specifications of the SSR models based on the Nelson-Siegel model by focusing on a trade-off between estimation performance and theoretical consistency. This paper highlights the importance of evaluating monetary policy easing effects using the entire yield curve fluctuations, rather than relying solely on SSR estimates, especially in the ultra-low interest rate environment in Japan.

Keywords: Effective lower bound constraint; Shadow short-term interest rates; Nelson-Siegel model; Monetary policy indicators.

JEL Classification codes: E43, E44, E52, G12.

1 Introduction

Shadow short-term interest rate (SSR) models are expected to provide effective monetary policy indicators under the effective lower bound (ELB) constraint on nominal interest rates. This paper revisits the SSR models using yield curve data from Japan's prolonged ultra-low interest rate environment. Specifically, this paper compares various specifications of the SSR models based on the Nelson-Siegel model by focusing on a trade-off between estimation performance and theoretical consistency.

The Japanese economy has recently escaped the ELB constraint on nominal interest rates for a prolonged period of 30 years since the mid-1990s (Figure 1),[1] restoring a financial environment with significantly positive interest rates from short- to long-term interest rates. However, in Japan's prolonged ultra-low interest rate environment, short-term interest rates remained near zero for about three decades since the Bank of Japan (BOJ) lowered its target for the overnight uncollateralized call rate (policy interest rate) to 0.5% in September 1995. Long-term interest rates, or 10-year Japanese Government Bond (JGB) yields, also followed a downward trend towards 2016 and remained near zero until early 2022.[2]

In the ultra-low interest rate environment in Japan, the BOJ implemented a wide range of unconventional monetary policy measures by both extending the scope of its interest rate policy and expanding the scale and range of large-scale asset purchases. Furthermore, since the Global Financial Crisis (GFC) of 2008, central banks in major advanced economies also faced the ELB constraint on nominal interest rates and launched large-scale unconventional monetary policies. Amidst accelerating inflation following the COVID-19 pandemic of 2020, major advanced economies, including Japan, returned to an interest rate policy. However, with equilibrium real interest rates remaining low, it is entirely conceivable that monetary policy operations will increasingly rely not only on adjustments to traditional policy rates, but also on unconventional monetary policy measures using central bank balance sheets.

Unconventional monetary policy faces the challenge that its stance is difficult to summarize in a single indicator. Under the ELB constraint on nominal interest rates, unconventional monetary policy encompasses a broad range of policy tools, including forward guidance, negative interest rates, yield curve control, and large-scale asset

---

[1] Shiratsuka (2025a) analyzes the yield curve dynamics under the prolonged ultra-low interest rate environment in Japan using the dynamic Nelson-Siegel models.

[2] The effective short-end of the yield curve shifts toward longer maturities, as a central bank implements unconventional monetary policy measures under the ELB constraint on the policy interest rate. In the next section, we examine how the prolonged ultra-low interest rate environment in Japan led to the tightening of the ELB constraint, affecting not only short-term but also medium- and long-term interest rates, following Swanson and Williams (2014).

Figure 1: Short- and Long-term Interest Rates in Japan
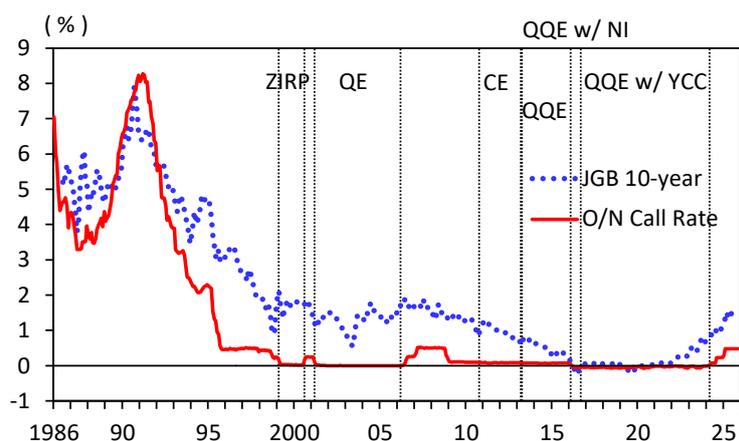
Notes: Abbreviations in the figures correspond to the monetary policy regime below: ZIRP, Zero Interest Rate Policy (February 1999–August 2000); QE, Quantitative Monetary Easing Policy (March 2001–March 2006); CE, Comprehensive Monetary Easing Policy (October 2010–March 2013); QQE, Quantitative and Qualitative Monetary Easing Policy (April 2013–March 2024); QQE w/ NI, Quantitative and Qualitative Monetary Easing Policy with Negative Interest Rate (February 2016–March 2024); QQE w/ YCC, Quantitative and Qualitative Monetary Easing Policy with Yield Curve Control (September 2016–March 2024).

Sources: Bank of Japan, Ministry of Finance.

purchase programs for a wide range of financial assets, not just JGBs but exchange-traded funds (ETFs) and Japan's real estate investment trusts (J-REITs). It is necessary to develop an indicator that integrates these diverse policy tools and comprehensively captures the stance of monetary policy. By contrast, conventional monetary policy practically gauges the policy stance through the level of the policy interest rate. Research has accumulated on policy rules linking this rate to macroeconomic indicators such as inflation and the output gap.

As a result of the above circumstances, the SSR models have attracted attention for providing monetary policy indicators that comprehensively capture the effects of unconventional monetary policy. By explicitly incorporating the ELB constraint on the policy interest rate, the SSR models enable to construct monetary policy indicators under the ELB constraint. For example, using the SSRs allows us to measure how low the rates would have fallen in the absence of the ELB constraint.

Looking at previous research on the SSR models, the starting point is a series of studies that incorporate the call option property of nominal interest rates, first proposed by Black (1995), into yield curve models. For example, Wu and Xia (2016) applied the SSR model to the US, estimated the SSR without the ELB constraint, and analyzed its relationship with macroeconomic variables. They argue that during periods of the ELB constraint, the SSR models provide a better indicator of the monetary policy stance than the federal funds rate.

2

The standard SSR models are based on finance theory and incorporate the no-arbitrage conditions, thereby accounting for the ELB constraint on interest rates.[3] Research on the SSR models, which extend yield curve models assuming the Gaussian affine term structure (GATS) model where short-term interest rates (risk-free instantaneous spot rates) follow Gaussian processes expressed as affine functions of state variables, includes, for example, Kim and Singleton (2012), Ichiue and Ueno (2013), Kim and Priebsch (2024), and Wu and Xia (2016). In addition, Christensen and Rudebusch (2015) and Krippner (2015) extend the dynamic Nelson-Siegel (DNS) model to incorporate the no-arbitrage condition and the ELB constraint.

We focus on the SSR models that assume the Nelson-Siegel (NS) model, proposed by Nelson and Siegel (1987), as their underlying yield curve model. The NS model assumes that daily yield curve fluctuations can be decomposed into three factors: level, slope, and curvature. While the NS model is static, the dynamic NS (DNS) model extends this analytical framework by incorporating time-varying parameters. Furthermore, Christensen et al. (2011) analytically demonstrate that the arbitrage-free Nelson-Siegel (AFNS) model, which incorporates the no-arbitrage condition into the DNS model, can be expressed by a simple formulation that adds a yield adjustment term (volatility term) to the DNS model. The B-AFNS model of Christensen and Rudebusch (2015) constructs the SSR model by incorporating the ELB constraint of Black (1995) on nominal interest rates in the AFNS model.[4]

In the US, as the ELB constraint on nominal interest rates tightened, affecting not only short-term but also medium- to long-term interest rates, Opschoor and van der Wel (2022) proposed the SSR model focusing on goodness-of-fit rather than theoretical consistency. Their model enhances the flexibility of the estimation framework by relaxing the no-arbitrage condition. Such an extension enables us to set the lower bound constraint on the spot rate rather than the instantaneous forward rate (IFR) and to make the loading parameters time-varying. Opschoor and van der Wel (2022) refer to this model as the "Smooth Shadow rate DNS (SB-DNS) model."[5] Opschoor and van der Wel (2022) compare this model with the conventional latent interest rate model, the B-AFNS model by Christensen and Rudebusch (2015). They demonstrate that even

---

[3] We categorize prior research into two types: (1) the assumption of the no-arbitrage condition in finance theory with the ELB constraint on nominal interest rates, and (2) priority on model fit and predictive accuracy without assuming specific theory. We conduct our analysis using the Black arbitrage-free Nelson-Siegel (B-AFNS) model as a representative of the former and the SB-DNS and SB-DNS-TVL models as representatives of the latter.

[4] The primary reason for using the B-AFNS model is its relatively low computational burden for the extended Kalman filter. While the Krippner arbitrage-free Nelson-Siegel (K-ANS) model by Krippner (2015) is also an NS-type SSR model, it employs an iterated extended Kalman filter, which tends to increase computational burden.

[5] The "shadow rate" concept is based on Black (1995), hence the inclusion of "B" in the abbreviation, with deepest appreciation to Black.

without considering the no-arbitrage condition, the SB-DNS model shows comparable goodness-of-fit and robustness (forecasting accuracy).

In this paper, we revisit the SSR models, using yield curve data from the prolonged ultra-low interest rate environment in Japan. To that end, we compare the various specifications of the SSR models, focusing on a trade-off between estimation performance and theoretical consistency in three respects: (1) Whether to assume the no-arbitrage condition; (2) Whether to fix a loading parameter or make it time-varying; and (3) Whether to adopt a 2- or 3-factor model as the yield curve model. This paper is the first to comprehensively evaluate multiple SSR models in the context of Japan's prolonged ultra-low interest rate environment. It thus provides guidance for SSR model selection and offers novel insights into monetary policy assessment under ultra-low interest rate conditions.

First, regarding the presence or absence of the no-arbitrage condition assumption, models with the no-arbitrage condition introduce an effective lower bound constraint on the IFR, because such models consider the no-arbitrage condition by starting with small changes in state variables based on Brownian motion. On the other hand, models without imposing the no-arbitrage condition focus more on the goodness-of-fit by introducing a lower bound constraint on yields themselves, rather than on IFRs. The models also assume that the variance of the observation error is constant. As pointed out by Krippner (2020), this is because in models with the no-arbitrage condition, if the variance of the observation error differs by maturity, the variances at the extremes (short-term and ultra-long-term) become large, leading to a poor goodness-of-fit. Conversely, models without no-arbitrage conditions often assume different variances for each observation error.

Second, regarding the time-varying loading parameter, models with the no-arbitrage condition are unable to make it time-varying because the conditional means and variances of the state variable are specified by the model parameters. In contrast, models without the no-arbitrage condition enable greater flexibility in model specification. For example, it is possible to make the loading parameter time-varying and introduce time-varying volatility in the error terms with the GARCH process, thereby further improving the goodness-of-fit.

Third, the NS model decomposes the fluctuations in the yield curve into three factors: level, slope, and curvature. However, when estimating the SSR models with no-arbitrage conditions, only two factors, level and slope, are typically used to reduce computational load and enhance the stability of the estimation results. Looking at the previous literature, the 3-factor model is recommended over the 2-factor model in terms of goodness-of-fit, as examined by Wu and Xia (2016), Kim and Priebsch (2024),

and Christensen and Rudebusch (2015). However, from a stability perspective, the 2-factor model is often recommended. Stability here refers to the stability of the estimation results with respect to the method of setting the effective lower bound on interest rates, differences in the estimation period, and the difference in the maturity structure of the interest rate data, as discussed by Krippner (2015).

Based on the estimation results of the SSR models, we construct three monetary policy indicators: the shadow short-term interest rate (SSR), the long-term forward rate (LFR), and the effective monetary stimulus (EMS). SSR and LFR are the short- and long-end of the shadow IFR curve, respectively. EMS is a measure of the extent to which the shadow IFR curve is pushed downward from LFR to a given maturity. Note that these monetary policy indicators capture the expected effects of monetary policy, as reflected in the the information on the yield curve. Under the ELB constraint, monetary policy management relies heavily on expectations management. Therefore, we aim to examine how expectations regarding the future path of monetary policy in financial markets evolve in response to changes in economic and financial conditions.

We empirically show that, in evaluating the monetary policy stance in Japan, SSR was a sufficient indicator prior to the GFC of 2008, because two factors, level and slope, adequately captured changes in the yield curve fluctuations. However, since then, the contribution of the curvature factor, which indicates medium- to long-term downward pressure on the yield curve, has become significant. Moreover, the stability of the level factor or LFR has been affected by the estimation model, as the entire yield curve has declined significantly.[6] Therefore, when evaluating the monetary policy stance, it has become increasingly important to consider the overall shape of the yield curve.

This paper is structured as follows. Section 2 empirically demonstrates the tightness of the ELB constraint on nominal interest rates in Japan, following Swanson and Williams (2014). Section 3 outlines the SSR models used in this paper. Section 4 explains the estimation method and data used to estimate the SSR models, presents the estimation results, and compares the model specifications. Section 5 proposes several monetary policy indicators and examines the differences in estimates across the specifications of SSR models using the estimation results in Section 4. Section 6 concludes this paper.

---

[6] Shiratsuka (2025a) points out that the parameters for the nonlinear functional form, defined as the Nelson-Siegel model, are difficult to estimate in a robust manner under the ultra-low interest rate environment in Japan. In particular, the estimates of the level and loading parameters are contaminated with each other, making it difficult to identify them precisely.

2 Tightening the Effective Lower Bound Constraint

In Japan, the ELB constraint has tightened due to the prolonged ultra-low interest rate environment, affecting not only short-term but also medium- to long-term interest rates. We first use the method of Swanson and Williams (2014) to confirm the maturity to which the ELB constraint tightened.

Swanson and Williams (2014) propose a method to measure the tightness of the ELB constraint not by focusing on the interest rate levels themselves, but by evaluating the sensitivity of interest rates to surprises in the releases of macroeconomic statistics. Specifically, they use professional forecasts for expected components and the difference between actual releases and professional forecasts for unexpected components, or surprises.[7]

We consider the equation below.

$$\Delta y_t = \alpha + \beta X_t + \varepsilon_t. \tag{1}$$

Here, Δy_t represents the daily change in the interest rate, X_t denotes the surprise components of macroeconomic macroeconomic data release, which is assumed to be related to interest rate fluctuations, β is the parameter, α is the constant term, and ε_t is the error term.[8]

When making estimations, macroeconomic data are published at various frequencies, such as monthly and quarterly, raising concerns about small sample bias. To address this issue, Swanson and Williams (2014) rewrite Equation (1) as Equation (2).

$$\Delta y_t = \gamma^i + \delta^i \beta X_t + \varepsilon_t. \tag{2}$$

Here, i denotes the year, and γ^i and δ^i are the constant and slope parameter for year i, respectively. β is a constant parameter throughout the estimation period.

δ^i represents sensitivity, and a significantly positive value indicates a significant reaction to news, suggesting that the ELB constraint is not binding. Since we are interested in the time-varying nature of δ^i, we first estimate Equation (2) using nonlinear maximum likelihood estimation to obtain parameter estimates. Then, using Equation

---

[7] More precisely, a surprise series is used, which normalizes the difference between the released data and the median of professional forecasts using the standard deviation of that time series.

[8] We use the following 15 surprise series available from Bloomberg ECO from 2010 to 2023: (1) unemployment rate, (2) core machinery orders (year-on-year), (3) consumer confidence index, (4) consumer price index (excluding fresh food/year-on-year, YoY hereafter), (5) producer price index (YoY), (6) gross domestic product (seasonally adjusted / Quarter-on-Quarter), (7) Monthly Labor Survey total cash earnings (YoY), (8) housing starts (annualized), (9) industrial production (YoY), (10) household expenditures (YoY), (11) current account balance, (12) trade balance (Balance of Payments Basis), (13) Tankan business fixed investment (YoY, large enterprises all industries), (14) Tankan business conditions (large manufacturing enterprises), (15) job openings-to-applicants ratio.

([3](#)) with these parameters substituted, we estimate the time-varying sensitivity δ^h using a rolling window of approximately one year.[9] Here, h denotes the rolling period.

$$\Delta y_t = \gamma^h + \delta^h \hat{X}_t + \varepsilon_t, \quad \hat{X}_t = \hat{\beta} X_t. \tag{3}$$

We set the estimation period from 2010 to 2023 and use the sensitivity from 2010 to 2012 (the pre-QQE period) as the benchmark period. We thus compare whether sensitivity δ^h declined thereafter by setting the average of δ over the first three years at one.

Figure [2](#) plots the time-varying estimates of δ. The key point here is the case where δ is significantly lower than one and insignificantly different from zero (the upper limit of the confidence interval is less than one and the lower limit is less than zero).[10] In this case, interest rate fluctuations are strongly affected by the ELB constraint.

The figure confirms that, in Japan, not only short-term interest rates but also medium- to long-term and ultra-long-term interest rates were strongly affected by the ELB constraint.[11] However, unlike Swanson and Williams (2014), we observe that the sensitivity was sometimes negative. It is important to note that sensitivity may be affected by factors specific to Japan, such as the low interest rates that prevailed during the benchmark period (the pre-QQE period) and the negative interest rates observed during certain periods.

3 Shadow Interest Rate Models

This section presents shadow interest rate models that explicitly consider the ELB constraint within the Nelson-Siegel framework.

## 3.1 Basic framework for the Nelson-Siegel model

In preparation for explaining the shadow interest rate models, we summarize the Nelson-Siegel (NS) model, proposed by Nelson and Siegel (1987), which is widely used in yield curve analysis.

---

[9] Since the one-year rolling window is approximately 250 business days, the estimations are repeatedly implemented using subsamples of 250 business days with 10-business-day intervals.

[10] Swanson and Williams (2014) conclude that if "H_0: $\delta^h = 0$" is accepted, the results are strongly affected by the effective lower bound constraint. However, in Japan, since the lower bound on nominal interest rates can be negative, it is important to note that cases where δ^h is significantly below zero are affected by the effective lower bound constraint.

[11] Shiratsuka (2025b) points out that the 10-year JGB yield had been strictly constrained by the YCC cap from mid-2022 to early 2023 due to speculative attacks. However, JGB yields at adjacent maturities, such as 7- and 30-year, are also insensitive to surprises in the releases of macroeconomic statistics, suggesting that the overall yield curve is highly constrained by the ELB during this period.

Figure 2: Time-varying Yield Sensitivity
to Surprises of Macroeconomic Data Releases
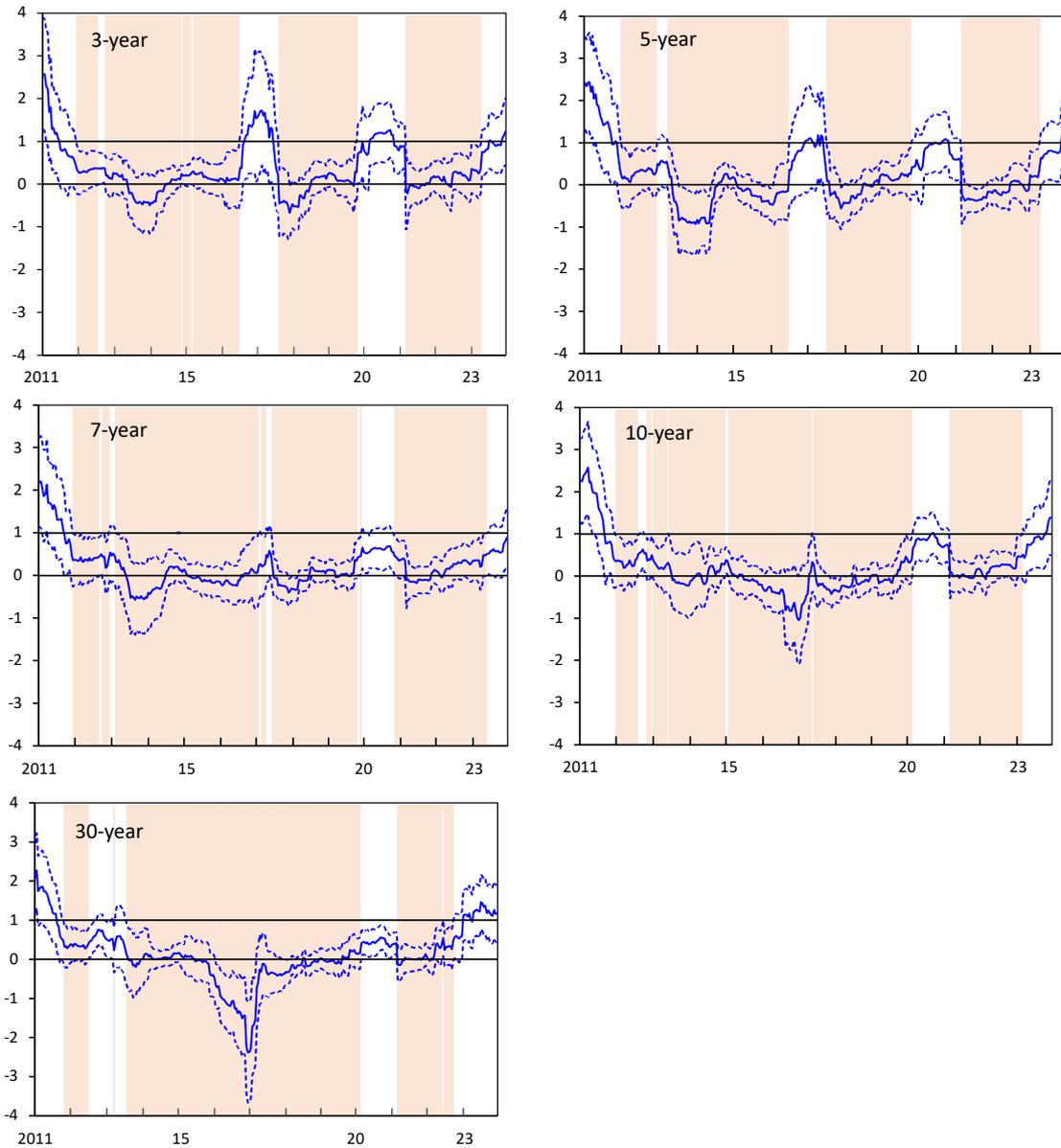
Notes: The estimations are repeatedly implemented using subsamples of 250 business days with 10-business-day intervals. The estimates of δ are normalized so that the average over the first three years equals one. The blue bold and dotted lines indicates the estimates and their 2-standard-error confidence intervals, respectively. The shaded areas indicate periods when the upper bound of the confidence interval for delta is below one, and the lower bound is below zero (indicating the estimates of δ have significantly decreased from the baseline). The solid horizontal lines correspond to values of one and zero, respectively, from top to bottom.

Nelson and Siegel (1987) describe the yield curve dynamics with three factors: level, slope, and curvature, supported by empirical studies. This model has simple and parsimonious functional forms but is flexible enough to capture the general property of the yield curve for monetary policy analyses. This model is applied in previous studies on the Japanese yield curve dynamics, such as Fujiki and Shiratsuka (2002), Okina and Shiratsuka (2004), Shiratsuka (2025a), and Shiratsuka (2025b).

The NS model specifies the IFR for the future period T in period t, denoted by $f(t, T)$, is given by

$$f(t,T) = L_t + S_t \exp(-\lambda_t(T-t)) + C_t\lambda_t(T-t)\exp(-\lambda_t(T-t)), \tag{4}$$

where L_t, S_t, and C_t correspond to the level, slope, and curvature factors, respectively. The variables for each factor are called factor loadings. λ_t is the loading parameter that determines the shape of the factor loadings and thereby controls the convergence speed toward a long-run level. All four parameters are estimated from the data. Among these parameters, L_t and λ_t are expected to take positive values.

The NS model has a property that the limits of forward rates when maturity approaches zero and infinity, respectively, are equal to $L_t + S_t$ and L_t. We exploit these two features to compile monetary policy indicators since it corresponds to the short- and long-end of the yield curve.

The IFR curve reflects market expectations of the future course of monetary policy or short-term interest rates and contains useful information for monetary policy-making. However, since spot rates are observed in financial markets, the NS model is estimated using spot rates. With the NS model, the spot rate $y(t, T)$ can be expressed as follows.

$$
\begin{aligned}
y(t,T) &= \frac{1}{T-t}\int_{m=t}^{T} f(t,m)dm \\
&= L_t + S_t\left(\frac{1-\exp(-\lambda_t(T-t))}{\lambda_t(T-t)}\right) + C_t\left[\left(\frac{1-\exp(-\lambda_t(T-t))}{\lambda_t(T-t)}\right) - \exp(-\lambda_t(T-t))\right].
\end{aligned}
\tag{5}
$$

$y(t, T)$ is obtained by integrating the forward rate, given by Equation (4), from period t to future period T and dividing by the time to maturity $(T - t)$.

The original and static NS model employs Equation (5) to estimate the yield curve at a single point in time. The dynamic NS (DNS) model extends it by assuming a dynamic process for the estimated parameters, thereby incorporating not only the cross-sectional dimension at a single point but also the time-series dimension.

Note that the B-AFNS model used in this paper introduces the ELB constraint on nominal interest rates into a DNS model with assuming no-arbitrage conditions. The SB-DNS model introduces the ELB constraint into a DNS model without assuming no-arbitrage conditions. The SB-DNS-TVL model further makes the loading parameter time-varying.

3.2 Basic concept of shadow interest rates

Next, we summarize the concept of the shadow interest rate model. This model is based on the idea proposed by Black (1995), which views the interest rate as a type of option. The model treats the nominal interest rate as a European call option, with the shadow interest rate as the underlying asset and the lower bound of the nominal interest rate as the strike price (Figure 3, referred to as the max function). That is, the short-term interest rate r_t, with its lower bound $r_{\min}$, can be expressed as follows:

Figure 3: Structure of European Call Options
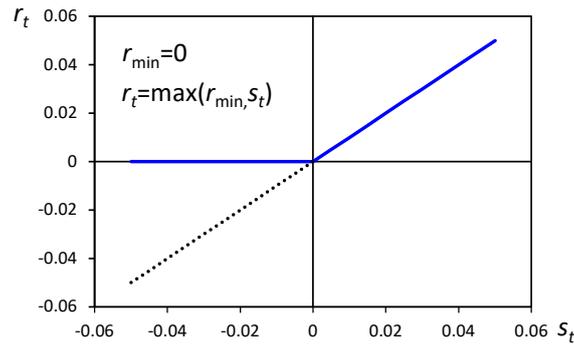
$$r_t = \max(r_{\min}, s_t) = s_t + \max(0, -s_t + r_{\min}) \tag{6}$$

Here, s_t is the shadow short-term interest rate (SSR).

The second term shows that the short-term interest rate can be interpreted as a call option with the shadow interest rate s_t as the underlying asset and $r_{\min}$ as the strike price. The third term indicates that the observed nominal interest rate equals the sum of the shadow interest rate and the option value, which prevents the short-term interest rate from falling below the lower bound. The model used in this paper follows this approach, decomposing a bounded interest rate into a shadow interest rate without a lower bound and an option value imposing the lower bound constraint.

Based on the above summary of the basic concepts of the NS model and the shadow interest rate model, we explain the shadow interest rate models used in this paper: the

B-AFNS model, which assumes the no-arbitrage condition, and the SB-DNS model and the SB-DNS-TVL model, which do not assume it.

3.3 B-AFNS model

First, we introduce the B-AFNS model as a shadow interest rate model that assumes the no-arbitrage condition. As mentioned above, the formulation in this paper is based on the B-AFNS model by Christensen and Rudebusch (2015), with reference also to the K-ANS model by Krippner (2015). The B-AFNS model can be expressed as a state-space model consisting of the following state and observation equations.

State equation

Let Θ_t denote the information set available at time t. Given this information, we consider the conditional expectations and variances of the state variables. Following Duffee (2002), the conditional expectation and conditional variance of the state variables in an affine model following a Gaussian process can be expressed as follows.[12]

$$E^p[X_T|\Theta_t] = (I - \exp(-K^P(T-t))\theta^P + \exp(-K^P(T-t))X_t, \qquad (7)$$

$$V^P[X_T|\Theta_t] = \int_{m=t}^{T} \exp(-K^P(T-m))\Sigma\Sigma' \exp(-K^{P'}(T-m))dm. \qquad (8)$$

Here, t denotes the current period, and T denotes a future period. Therefore, the conditional moments of the discretioned observations can be expressed in VAR(1) form as follows.

$$X_t = (I - \exp(-K^p\Delta t))\theta^P + \exp(-K^p\Delta t)X_{t-1} + \eta_t. \qquad (9)$$

This expression is the state equation for the extended Kalman filter. The parameters for the 2-factor and the 3-factor models are given as follows.

$$X_t = \begin{pmatrix} L_t \\ S_t \end{pmatrix}, \quad K^P = \begin{pmatrix} k_{11}^P & k_{12}^P \\ k_{21}^P & k_{22}^P \end{pmatrix}, \quad \theta^P = \begin{pmatrix} \theta_1^P \\ \theta_2^P \end{pmatrix}, \qquad (10)$$

$$X_t = \begin{pmatrix} L_t \\ S_t \\ C_t \end{pmatrix}, \quad K^P = \begin{pmatrix} k_{11}^P & k_{12}^P & k_{13}^P \\ k_{21}^P & k_{22}^P & k_{23}^P \\ k_{31}^P & k_{32}^P & k_{33}^P \end{pmatrix}, \quad \theta^P = \begin{pmatrix} \theta_1^P \\ \theta_2^P \\ \theta_3^P \end{pmatrix} \qquad (11)$$

---

[12] The conditional expectation of this factor X becomes the state equation, and its conditional variance becomes the variance-covariance matrix of the state equation. Therefore, note that, unlike the DNS models, the variance-covariance matrix is constructed from the model parameters.

X_t represents the factors (level L, slope S, curvature C). Δt is the data frequency, and $\Delta t = 1/12$ in this paper, since the monthly data are used. η_t is the error term.

Observation equation

The observation equation (cross-section) is defined for spot rates observed in financial markets and therefore requires considering interest rates with a lower bound. Equations (4) and (5) assume no lower bounds for the IFR and spot rate. We define the IFR and the spot rate with a lower bound by adding an under-bar to these symbols, $\underline{f}$ and $\underline{y}$, respectively. Since the spot rate is the average of the IFR over the period until maturity, the following relationship holds between the spot rate and the IFR in the B-AFNS model:

$$\underline{y}(t,T) = \frac{1}{T-t} \int_{m=t}^{T} \underline{f}(t,m)dm + \varepsilon_t \tag{12}$$

Here, ε_t represents the error term. The IFR with a lower bound consists of the IFR without a lower bound $f(t,T)$ and an optional term $z(t,T)$ as follows.

$$\underline{f}(t,T) = f(t,T) + z(t,T) \tag{13}$$

To differentiate from the lower-bound-constrained IFR, we refer to the IFR without considering the lower bound as the shadow IFR. The shadow IFR is given by the following equation in the two- and 3-factor models.

$$f(t,T) = L_t + S_t \exp(-\lambda_t(T-t)) + VE(t,T), \tag{14}$$

$$f(t,T) = L_t + S_t \exp(-\lambda_t(T-t)) + C_t\lambda_t(T-t)\exp(-\lambda_t(T-t)) + VE(t,T). \tag{15}$$

The volatility effect $VE(t,T)$ is derived from the no-arbitrage condition. It is a function that takes negative values, expressed in terms of the maturity $(T-t)$, the loading parameter λ_t, and the volatility (variance and covariance) of the state equation. Although it varies with maturity, it remains constant at each maturity over time.[13]

Following Christensen and Rudebusch (2015) by applying the quasi-analytical solution from Krippner (2012), the option term can be expressed as follows,

---

[13] This term is referred to as the Jensen term (yield adjustment term). The Jensen term captures convexity, which corrects for the nonlinearity between interest rates and prices, and it takes negative values. When using interest rate data up to a 10-year maturity, the Jensen term is small and can be safely ignored. However, note that this paper uses interest rate data up to a 30-year maturity, resulting in a large Jensen term that must be included in the shadow IFR.

$$z(t, T) = (r_{\min} - f(t, T)) \left(1 - \Phi \left(\frac{f(t, T) - r_{\min}}{\omega(t, T)} \right) \right) + \omega(t, T) \frac{1}{\sqrt{2\pi}} \exp \left(-\frac{1}{2} \left[\frac{f(t, T) - r_{\min}}{\omega(t, T)} \right]^2 \right).$$

$$(16)$$

The lower-bound-constrained IFR is given by

$$\underline{f}(t, T) = r_{\min} + (f(t, T) - r_{\min}) \Phi \left(\frac{f(t, T) - r_{\min}}{\omega(t, T)} \right) + \omega(t, T) \frac{1}{\sqrt{2\pi}} \exp \left(-\frac{1}{2} \left[\frac{f(t, T) - r_{\min}}{\omega(t, T)} \right]^2 \right)$$

$$(17)$$

Here, Φ denotes the cumulative distribution function for the standard normal distribution and $\omega(t, T)^2$ represents the variance of the shadow IFR, excluding the volatility effect.[14] The above equations constitute the formulation of the observation equation.

The short-term interest rate is expressed as follows.

$$r_t = \max(r_{\min}, s_t), \quad s_t = L_t + S_t \qquad (18)$$

Here, s_t is the shadow IFR at maturity zero, referred to as the shadow interest rate.[15] Therefore, the nominal interest rate in Equation (18) can be interpreted as a call option defined on the shadow short-term interest rate s_t with strike price $r_{\min}$.

3.4 SB-DNS model and SB-DNS-TVL model

Next, we illustrate the SB-DNS and SB-DNS-TVL models by Opschoor and van der Wel (2022) as shadow interest rate models without assuming the no-arbitrage condition.[16] The difference from the B-AFNS model is that, while the B-AFNS model imposes a lower bound constraint on the IFR, as shown in equation (17), the SB-DNS and SB-DNS-TVL models impose a lower bound constraint on the spot rate.

We use the following functional form to impose lower bounds on both models.[17]

---

[14] Note that Equation (17) is not an analytical solution in the strict sense, but rather a quasi-analytical solution, as it relies on the standard normal cumulative distribution function.

[15] Note that at maturity zero, the VE term becomes zero, so the shadow IFR is equal to the future course of the shadow interest rate.

[16] Note that Opschoor and van der Wel (2025), unlike Opschoor and van der Wel (2022), do not treat the loading parameters as time-varying. This modification is likely based on the findings of van Dijk et al. (2014) and Christensen and Rudebusch (2019), which suggest that the sharp decline followed by rapid rebound of the equilibrium real interest rate in the United States is better explained by a shift in level rather than changes in the factor loadings of slope and curvature. In contrast, for Japan, as the room for long-term interest rates to decline diminishes, studies such as Koeda and Sekine (2022) and Shiratsuka (2025a) point out that incorporating a decaying loading parameter (decay factor) better captures the shape of the yield curve.

[17] When $\omega = 1$, $r_{\min} = 0$, and $x = z$, this equation corresponds to $f_G(x) = x\Phi(x) + \phi(x)$ in Opschoor and van der Wel (2025).

$$\underline{y} = r_{\min} + ((z - r_{\min})\Phi(Z) + \omega\phi(Z)), \quad Z = \frac{z - r_{\min}}{\omega} \qquad (19)$$

Here, Φ denotes the cumulative distribution function of the standard normal distribution, ϕ denotes the probability density function of the standard normal distribution, and ω denotes the standard deviation of the future path. In Equation (19), when $\omega = 0$, it becomes equivalent to the max function expressed in Equation (18).

Figure 4 depicts the shape obtained by varying ω in Equation (19) with $r_{\min} = 0$ and $z = [-0.05, 0.05]$. As ω increases, the shape becomes smoother than that of the max function, thus the model is termed "Smooth Shadow rate DNS."[18] As clearly shown in the figure, a larger ω makes the lower bound constraint more binding on both short-term and medium-to-long-term interest rates. Therefore, ω can be interpreted as representing the tightness of the ELB constraint.

Figure 4: Functional Form
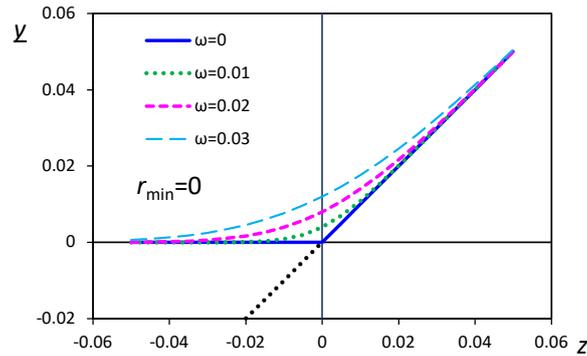
Notes: The figure depicts the shape of the function, described as Equation (19), when $r_{\min} = 0$, $z = [-0.05, 0.05]$, and ω is given exogenously. The horizontal and vertical axes represent maturity and yield, respectively.

Note that the B-AFNS model and the SB-DNS and SB-DNS-TVL models make different assumptions regarding ω. The B-AFNS model determines ω based on its model parameters and assigns different values to each maturity. In contrast, the SB-DNS and SB-DNS-TVL models take a constant value throughout all maturities. Furthermore, the SB-DNS and SB-DNS-TVL models estimate ω, thus improving the fit of the model compared to the B-AFNS model.

The SB-DNS and SB-DNS-TVL models can also be expressed as state-space models consisting of a state equation and an observation equation, as in the B-AFNS model.

---

[18] However, as mentioned above, while the B-AFNS model, K-ANSM, and the model by Wu and Xia (2016) are not explicitly termed "smooth," it is important to note that since ω is not zero, their shapes are smoother than those of the max function.

State equation

The state equations of the SB-DNS model can be expressed in VAR(1) form as follows.

$$X_t = (I - F)\mu + FX_{t-1} + \eta_t. \tag{20}$$

The model parameters for the two- and 3-factor models are as follows, respectively.

$$X_t = \begin{pmatrix} L_t \\ S_t \end{pmatrix}, \quad F = \begin{pmatrix} \phi_{11} & \phi_{12} \\ \phi_{21} & \phi_{22} \end{pmatrix}, \quad \mu = \begin{pmatrix} \mu_1 \\ \mu_2 \end{pmatrix}, \tag{21}$$

$$X_t = \begin{pmatrix} L_t \\ S_t \\ C_t \end{pmatrix}, \quad F = \begin{pmatrix} \phi_{11} & \phi_{12} & \phi_{13} \\ \phi_{21} & \phi_{22} & \phi_{23} \\ \phi_{31} & \phi_{32} & \phi_{33} \end{pmatrix}, \quad \mu = \begin{pmatrix} \mu_1 \\ \mu_2 \\ \mu_3 \end{pmatrix}. \tag{22}$$

In addition, η_t is the error term.

The state equations of the SB-DNS-TVL model can also be expressed as a VAR(1) model by adding the factor element λ_t to the SB-DNS model. The model parameters for the two- and 3-factor models are as follows, respectively.

$$X_t = \begin{pmatrix} L_t \\ S_t \\ \lambda_t \end{pmatrix}, \quad F = \begin{pmatrix} \phi_{11} & \phi_{12} & \phi_{13} \\ \phi_{21} & \phi_{22} & \phi_{23} \\ \phi_{31} & \phi_{32} & \phi_{33} \end{pmatrix}, \quad \mu = \begin{pmatrix} \mu_1 \\ \mu_2 \\ \mu_3 \end{pmatrix}, \tag{23}$$

$$X_t = \begin{pmatrix} L_t \\ S_t \\ C_t \\ \lambda_t \end{pmatrix}, \quad F = \begin{pmatrix} \phi_{11} & \phi_{12} & \phi_{13} & \phi_{14} \\ \phi_{21} & \phi_{22} & \phi_{23} & \phi_{24} \\ \phi_{31} & \phi_{32} & \phi_{33} & \phi_{34} \\ \phi_{41} & \phi_{42} & \phi_{43} & \phi_{44} \end{pmatrix}, \quad \mu = \begin{pmatrix} \mu_1 \\ \mu_2 \\ \mu_3 \\ \mu_4 \end{pmatrix}. \tag{24}$$

Observation equation

The observation equation of the SB-DNS and SB-DNS-TVL models set a lower bound directly on the spot rate, rather than imposing a lower bound constraint on the IFR as in models considering the no-arbitrage condition. Specifically, it derives the following spot rate with a lower bound by replacing the IFR in Equation (17) with the spot rate.

$$\underline{y}(t, T) = r_{\min} + (y(t, T) - r_{\min})\Phi\left(\frac{y(t, T) - r_{\min}}{\omega}\right) + \omega \frac{1}{\sqrt{2\pi}} \exp\left(-\frac{1}{2}\left[\frac{y(t, T) - r_{\min}}{\omega}\right]^2\right) + \varepsilon_t. \tag{25}$$

4   Estimation of the SSR Models

In this section, we estimate six specifications of the SSR models and examine model selection for computing monetary policy indicators.

4.1   Data and estimation methods

4.1.1   Data

We use eight series of JGB zero-coupon yields, computed by Bloomberg, with maturities of 6-month, 1-, 2-, 3-, 5-, 7-, 10-, and 30-year to estimate the B-AFNS, SB-DNS, and SB-DNS-TVL models.[19] The estimation period ranges from January 1995 to December 2024, using end-of-month data. Figure 5 plots the data used in the estimation.

Figure 5: JGB Yields
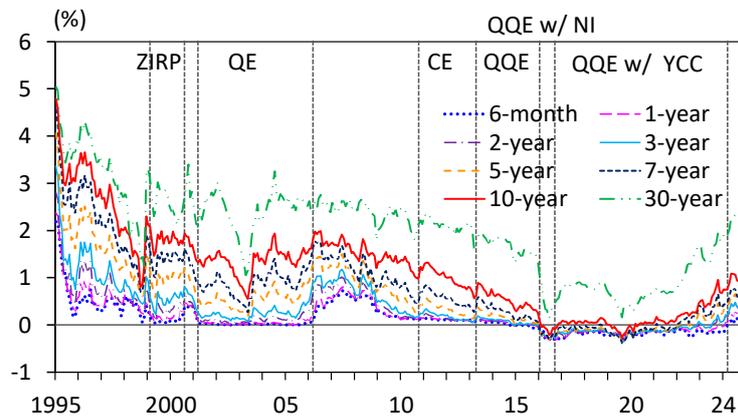
Notes: Regarding the abbreviations for the monetary policy regime, see the notes for Figure 1.
Source: Bloomberg.

4.1.2   Estimation methods

We employ an extended Kalman filter for the estimation. The extended Kalman filter is an extension of the Kalman filter that handles the nonlinear observation equation. It sequentially performs a prediction step, forecasting the next period based on observations up to time $(t-1)$, followed by an update step, which calculates the prediction error and its variance, then updates the prior prediction. This process estimates parameters that maximize the computed log-likelihood.

The error terms in the state and observation equations are assumed to follow the following distribution.

---

[19] The 3-month maturity is excluded from estimation due to its high volatility and different trends compared to other maturities. However, we confirm that including the 3-month maturity does not alter the implications derived from the estimation results in this paper.

$$\begin{pmatrix} \eta_t \\ \varepsilon_t \end{pmatrix} \sim WN \left[\begin{pmatrix} 0 \\ 0 \end{pmatrix}, \begin{pmatrix} Q & 0 \\ 0 & H \end{pmatrix} \right], \quad E\left[X_0\eta_t^{'}\right] = 0, \quad E\left[X_0\varepsilon_t^{'}\right] = 0. \qquad (26)$$

Here, Q is off-diagonal, and H is diagonal ($H = \text{diag}(s_1, s_2, ..., s_8)$). The error terms in the state and observation equations are assumed to be orthogonal to the initial values of the state variables.

In addition, elements of H take the same value at each time step in the B-AFNS model ($s_1 = s_2 = ... = s_8$), whereas they are assumed to differ across maturities in the SB-DNS and SB-DNS-TVL models.[20] The structure of Q is specified as follows in the B-AFNS model, based on the conditional variance of the state variables in the affine model following a Gaussian process, as shown the equation below.[21]

$$Q = \int_{m=t}^{T} \exp(-K^P(T-m)))\Sigma\Sigma' \exp(-K^{P'}(T-m))dm. \qquad (27)$$

In SB-DNS and SB-DNS-TVL models, Q is given by the equation below.

$$Q = \Sigma\Sigma'. \qquad (28)$$

Here, Σ is lower triangular, and the number of elements in each row and column matches the number of estimated factors, including loading parameters. In this case, the two-element specification includes B-AFNS(2) and SB-DNS(2), the three-element specification includes B-AFNS(3), SB-DNS(3), and SB-DNS-TVL(2), and the four-element specification includes SB-DNS-TVL(3).

Thus, $\Sigma\Sigma'$ for SB-DNS-TVL(3), which has the maximum number of elements, is a symmetric matrix, specified as follows:

$$\Sigma\Sigma' = \begin{pmatrix} \sigma_1^2 & \rho_{12}\sigma_1\sigma_2 & \rho_{13}\sigma_1\sigma_3 & \rho_{14}\sigma_1\sigma_4 \\ \rho_{12}\sigma_1\sigma_2 & \sigma_2^2 & \rho_{23}\sigma_2\sigma_3 & \rho_{24}\sigma_2\sigma_4 \\ \rho_{13}\sigma_1\sigma_3 & \rho_{23}\sigma_2\sigma_3 & \sigma_3^2 & \rho_{34}\sigma_3\sigma_4 \\ \rho_{14}\sigma_1\sigma_4 & \rho_{24}\sigma_2\sigma_4 & \rho_{34}\sigma_3\sigma_4 & \sigma_4^2 \end{pmatrix}, \qquad (29)$$

where $-1 < \rho_{ij} < 1$.

Based on the examination above, the number of estimated parameters for each specification is summarized in Table 1.

---

[20] We assume the error term in the observation equation is identical for all maturities in the B-AFNS model, but the standard deviation of the future path varies by maturity. Conversely, for the SB-DNS and SB-DNS-TVL models, the error term in the observation equation varies by maturity, but the standard deviation of the future path is identical for all maturities.

[21] Using the method of Fisher and Gilles (1996) for calculating Q reduces the computational load of integration.

Table 1: Number of Estimated Parameters

	B-AFNS		SB-DNS		SB-DNS-TVL	
	2-factor	3-factor	2-factor	3-factor	2-factor	3-factor
λ	1	1	1	1	—	—
K	4(=2x2)	9(=3X3)	4(=2x2)	9(=3X3)	9(=3X3)	16(=4X4)
θ	2	3	2	3	3	4
Σ	3	6	3	6	6	10
(σ)	(2)	(3)	(2)	(3)	(3)	(4)
(ρ)	(1)	(3)	(1)	(3)	(3)	(6)
s	1	1	8	8	8	8
ω	—	—	1	1	1	1
Total	11	20	19	28	27	39

4.1.3 Lower bound settings

Regarding the lower bound settings, we follow the procedure outlined by Kortela (2016). First, four candidate settings for the lower bound were considered: (1) a constant 0%, (2) a constant -0.1%, (3) the cumulative minimum (CM) of the policy interest rate up to each point in time, and (4) the minimum spot rate at each point in time (yield minimum). These settings were then compared based on whether the model's lower bound fell below the lower bound, whether the Akaike information criterion (AIC), root mean squared error (RMSE), and mean absolute error (MAE) for each maturity were small, whether they were consistent with yield indicators, and whether they effectively captured fluctuations in the medium- to long-term spot rates.

The result of the above verification procedure led us to consider changing the level of ELB as follows: (1) 0.15% for the period before February 1999 (end of January), (2) 0% for the period on or from February 1999 to September 2014, (3) yield minimum for the period on or after October 2014 to February 2024, and (4) 0% after March 2024.[22]

4.2 Estimation Results

4.2.1 Estimated parameters and goodness-of-fit

The estimates for six specifications of the SSR models are summarized in Table 2.[23]

Looking at the estimated values of the loading parameter λ, the 2-factor mod-

---

[22] Regarding changes to the method for setting the interest rate floor, the 3-factor model tends to exhibit a smaller overall impact and higher robustness.

[23] For the B-AFNS model, the 2-factor and 3-factor specifications are denoted by B-AFNS(2) and B-AFNS(3), respectively, and the SB-DNS and SB-DNS-TVL models are denoted similarly.

Table 2: Estimation Results

	B-AFNS(2)		B-AFNS(3)		SB-DNS(2)		SB-DNS(3)		SB-DNS-TVL(2)		SB-DNS-TVL(3)	
	Coef.	S.E.	Coef.	S.E.	Coef.	S.E.	Coef.	S.E.	Coef.	S.E.	Coef.	S.E.
λ	0.1134	0.0040	0.1528	0.0038	0.2177	0.0069	0.4162	0.0099	—	—	—	—
κ_{11}	-0.8341	0.0475	3.2597	0.2060	1.0118	0.0100	0.9818	0.0090	0.9305	0.0180	0.9345	0.0194
κ_{12}	-2.4012	0.1781	1.6504	0.1211	0.0225	0.0173	-0.0021	0.0122	0.0048	0.0130	-0.0056	0.0524
κ_{13}	—	—	-0.9141	0.0540	—	—	0.0266	0.0055	0.0011	0.0003	0.0219	0.0085
κ_{14}	—	—	—	—	—	—	—	—	—	—	0.0013	0.0004
κ_{21}	1.1377	0.0683	-1.2985	0.1468	-0.0704	0.0172	-0.0287	0.0158	-0.0699	0.0320	-0.0182	0.0453
κ_{22}	3.2065	0.2487	0.0166	0.0042	0.8756	0.0251	0.9095	0.0244	0.8813	0.0230	0.9266	0.0279
κ_{23}	—	—	0.5447	0.0289	—	—	-0.0053	0.0079	0.0017	0.0005	-0.0033	0.0220
κ_{24}	—	—	—	—	—	—	—	—	—	—	0.0004	0.0009
κ_{31}	—	—	-5.7069	0.2560	—	—	0.0280	0.0165	2.2703	0.7546	-0.1879	0.0633
κ_{32}	—	—	-3.8599	0.1785	—	—	-0.0120	0.0168	0.9202	0.5720	-0.1519	0.0697
κ_{33}	—	—	1.3871	0.1234	—	—	0.9384	0.0132	0.9574	0.0132	0.9333	0.0344
κ_{34}	—	—	—	—	—	—	—	—	—	—	0.0034	0.0020
κ_{41}	—	—	—	—	—	—	—	—	—	—	3.5668	1.5013
κ_{42}	—	—	—	—	—	—	—	—	—	—	2.2636	1.5655
κ_{43}	—	—	—	—	—	—	—	—	—	—	0.5028	0.5891
κ_{44}	—	—	—	—	—	—	—	—	—	—	0.9334	0.0491
θ_1	0.0638	0.0047	0.0767	0.0056	0.0776	0.0049	0.0601	0.0025	0.0535	0.0032	0.0506	0.0036
θ_2	-0.0619	0.0046	-0.0731	0.0056	-0.0691	0.0045	-0.0466	0.0037	-0.0540	0.0052	-0.0368	0.0068
θ_3	—	—	0.0332	0.0029	—	—	-0.0015	0.0077	-0.0741	0.0715	-0.0341	0.0209
θ_4	—	—	—	—	—	—	—	—	—	—	0.2033	0.3064
σ_{11}	0.0274	0.0011	0.0282	0.0010	0.0031	0.0002	0.0021	0.0002	-0.0023	0.0002	0.0022	0.0002
σ_{22}	0.0387	0.0014	0.0226	0.0011	0.0042	0.0003	0.0033	0.0003	0.0050	0.0006	0.0028	0.0002
σ_{33}			0.0528	0.0038	—	—	0.0066	0.0005	-0.1363	0.0089	0.0081	0.0009
σ_{44}	—	—	—	—	—	—	—	—	—	—	0.1209	0.0178
ρ_{12}	-0.9804	0.0019	-0.9072	0.0006	-0.7175	0.0375	-0.5176	0.0732	-0.0849	0.0738	-0.4522	0.1241
ρ_{13}	—	—	-0.7988	0.0058	—	—	-0.4222	0.0884	-0.3640	0.0997	0.1508	0.1888
ρ_{14}	—	—	—	—	—	—	—	—	—	—	-0.4631	0.1697
ρ_{23}	—	—	0.5844	0.0096	—	—	0.1679	0.1037	-0.3310	0.0561	-0.0455	0.1337
ρ_{24}	—	—	—	—	—	—	—	—	—	—	0.0147	0.0397
ρ_{34}	—	—	—	—	—	—	—	—	—	—	-0.7175	0.0674
s_1	9.15E-04	1.35E-05	5.06E-04	7.99E-06	7.30E-04	2.96E-05	1.86E-07	6.82E-10	6.46E-04	3.13E-05	4.48E-04	2.06E-05
s_2	—	—	—	—	4.91E-04	2.12E-05	2.50E-08	1.71E-10	4.09E-04	1.85E-05	2.01E-04	1.30E-05
s_3	—	—	—	—	-2.48E-04	1.48E-05	8.63E-08	3.19E-10	2.21E-04	1.63E-05	2.18E-04	1.13E-05
s_4	—	—	—	—	1.94E-04	1.24E-05	4.84E-08	4.23E-10	2.03E-04	1.13E-05	1.48E-04	9.39E-06
s_5	—	—	—	—	-1.94E-04	1.35E-05	3.68E-08	6.03E-10	1.77E-04	1.90E-05	1.36E-04	1.36E-05
s_6	—	—	—	—	-3.29E-04	2.32E-05	3.01E-07	1.49E-09	4.45E-04	2.26E-05	4.58E-04	2.07E-05
s_7	—	—	—	—	1.21E-03	5.55E-05	5.10E-08	3.44E-09	7.79E-04	5.41E-05	5.15E-04	5.10E-05
s_8	—	—	—	—	5.86E-03	2.49E-04	1.33E-05	1.14E-08	2.57E-03	2.34E-04	1.61E-03	1.59E-04
ω	—	—	—	—	0.0114	0.0007	0.0118	0.0009	0.0215	0.0018	0.0122	0.0012

els show smaller values than the 3-factor models.[24]   Generally, as λ decreases, the weighting in the factor loadings increases towards longer maturities. Therefore, the 3-factor models capture the downward pressure effect in the medium-to-long-term zone through the curvature term, whereas the 2-factor models, without the curvature term, capture it through a smaller loading parameter, resulting in a more gradual downward pressure effect via the slope term and exhibiting a more gradual upward-sloping shape of the yield curve.

However, the other estimated parameters of the SSR models themselves are rather difficult to interpret. We thus compare the estimation performance of the SSR models based on goodness-of-fit in two respects: standardized statistics and deviations between observed and estimated spot rates for selected maturities.

Table 3 shows the goodness-of-fit for six specifications. First, based on the log-likelihood, AIC, and BIC,[25] the SB-DNS and SB-DNS-TVL models, which do not impose the no-arbitrage condition, show a better fit than the B-AFNS models, which impose the no-arbitrage condition. Comparing the estimation results of the 2-factor and 3-factor models, the 3-factor models show a better fit.

Second, focusing on RMSE and MAE, 3-factor specifications are smaller than the corresponding 2-factor specifications. Among 3-factor specifications, SB-DNS-TVL(3) consistently shows high precision across maturities, except for 30-year. B-AFNS(3) also shows relatively high precision, especially for 30-year maturity.[26] However, for the 30-year maturity, the models incorporating the no-arbitrage condition, especially B-AFNS(3), have smaller RMSE and MAE. When considering the application to monetary policy indicators, it is worth noting that the overall goodness-of-fit and the goodness-of-fit for the 30-year spot rate do not necessarily coincide.

4.2.2   Estimated yield curve factors

Figure 6 shows the estimated yield curve factors of the level, slope, and curvature factors and the loading parameter, respectively, for the B-AFNS, SB-DNS, and SB-DNS-

---

[24]Estimates of the loading parameter λ are shown only for the B-AFNS and SB-DNS models for the fixed loading parameter specifications.

[25]AIC and BIC are defined as follows:

$$AIC = -\frac{2}{T} \times \text{log-likelihood} + \frac{2N}{T}, \quad BIC = -\frac{2}{T} \times \text{log-likelihood} + \frac{Nln(N)}{T},$$

where T and N indicate sample size and number of parameters, respectively.

[26]RMSE and MAE are defined as follows:

$$RMSE = \sqrt{\frac{1}{T} \sum_{t=1}^{T} (y_i - \hat{y}_i)^2}, \quad MAE = \frac{1}{T} \sum_{t=1}^{T} |y_i - \hat{y}_i|,$$

where T and N indicate sample size and number of parameters, respectively.

Table 3: Comparison of Goodness-of-Fit

	B-AFNS		SB-DNS		SB-DNS-TVL	
	(2)	(3)	(2)	(3)	(2)	(3)
# param.	11	20	19	28	27	39
AIC	-85.61	-92.54	-92.08	-96.02	-94.39	-97.78
BIC	-85.49	-92.33	-91.87	-95.72	-94.10	-97.36
Log-likelihood	1,5421.1	1,6677.9	1,6592.6	1,7311.5	1,7017.2	1,7639.1
RMSE						
6-month	0.089	0.058	0.072	0.041	0.063	0.042
1-year	0.076	0.032	0.048	0.012	0.039	0.017
2-year	0.074	0.039	0.022	0.028	0.019	0.020
3-year	0.061	0.044	0.015	0.019	0.017	0.011
5-year	0.056	0.037	0.014	0.014	0.012	0.008
7-year	0.099	0.045	0.026	0.053	0.040	0.043
10-year	0.092	0.055	0.116	0.011	0.071	0.043
30-year	0.107	0.022	0.577	0.357	0.231	0.134
Mean	0.082	0.042	0.111	0.067	0.061	0.040
MAE						
6-month	0.059	0.042	0.050	0.029	0.044	0.029
1-year	0.056	0.023	0.035	0.008	0.029	0.012
2-year	0.054	0.026	0.018	0.019	0.015	0.014
3-year	0.047	0.032	0.011	0.014	0.012	0.009
5-year	0.041	0.029	0.012	0.010	0.010	0.007
7-year	0.071	0.034	0.019	0.040	0.029	0.033
10-year	0.070	0.042	0.094	0.007	0.054	0.033
30-year	0.073	0.016	0.489	0.286	0.159	0.095
Mean	0.059	0.030	0.091	0.052	0.044	0.029

Notes: AIC, BIC, RMSE, and MAE are defined as follows:

$$AIC = -\frac{2}{T} \times \text{log-likelihood} + \frac{2N}{T}, \quad BIC = -\frac{2}{T} \times \text{log-likelihood} + \frac{Nln(N)}{T},$$

$$RMSE = \sqrt{\frac{1}{T}\sum_{t=1}^{T}(y_i - \hat{y}_i)^2}, \quad MAE = \frac{1}{T}\sum_{t=1}^{T}|y_i - \hat{y}_i|,$$

where T and N indicate sample size and number of parameters, respectively.

TVL models for both 2-factor (level, slope, and loading parameter only) and 3-factor (level, slope, curvature, and loading parameter) specifications.

The upper panel of the figure shows that the level factors in all specifications follow a gradual downward trend. However, during the period of the negative interest rate policy since February 2016, the estimates of the B-AFNS and SB-DNS models with the fixed loading parameter exhibit a significant decline, while those of the SB-DNS-TVL model with the time-varying loading parameter remain relatively stable at a high level. The above difference depends on whether the flattening of the yield curve under the negative interest rate policy is interpreted as a decline in the level itself or as a slower convergence speed toward the long-term level, as examined later.
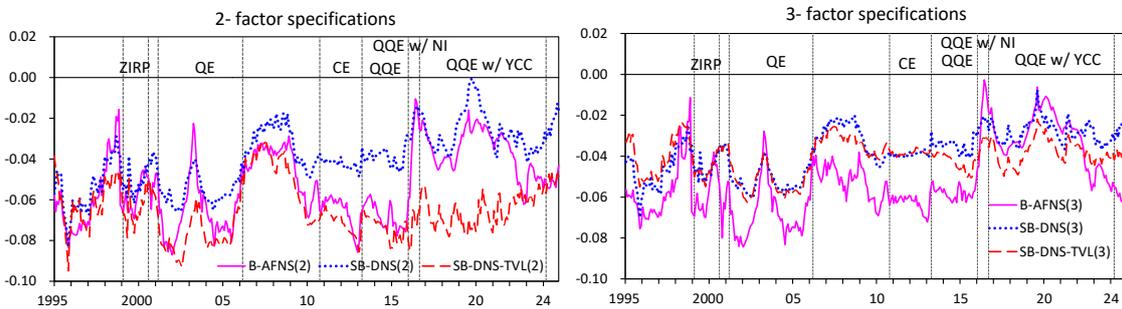
The middle panel of the figure indicates that the slope factors for the 2-factor speci-

Figure 6: Estimated Yield Curve Factors and Loading Parameter
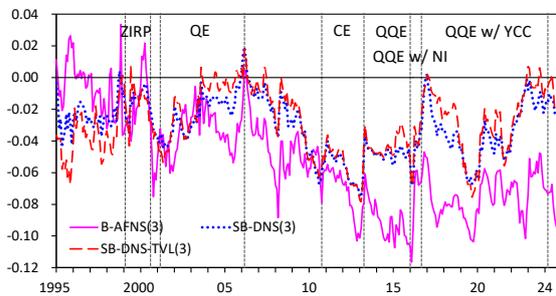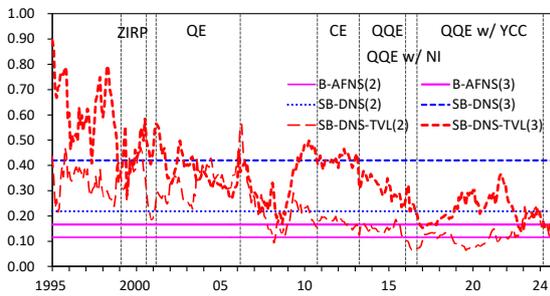
(1) Level factor
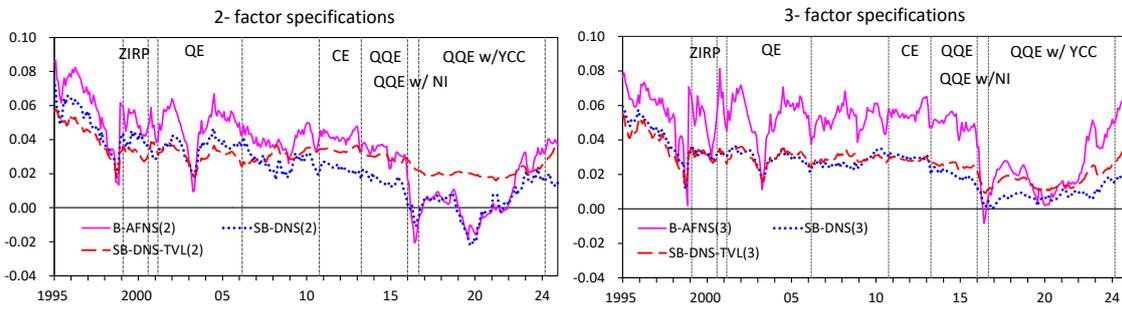
(2) Slope factor

(3) Curvature factor   (4) Loading parameter

Notes: Regarding the abbreviations for the monetary policy regime, see the notes for Figure 1.

fications generally exhibit greater negativity than for the 3-factor specifications. How-
ever, during the period of the negative interest rate policy, SB-DNS-TVL(2), the 2-factor
specification with time-varying loading parameters, shows a more negative slope fac-
tor, combined with a relatively high level factor. In contrast, the other 2-factor spec-
ifications with fixed loading parameters show a smaller negative slope factor with a
lower level factor.

The bottom left panel of the figure shows that the curvature factors generally fol-
low a similar trend before the introduction of the negative interest rate policy in 2016.
However, since then, estimates for B-AFNS(3) remain lower than those for the other

models. In addition, they show slightly more volatile movements.

The bottom right panel of the figure plots the estimated loading parameters over time. The estimates are smaller in the 2-factor specification than in the 3-factor specification, regardless of whether with fixed or time-varying loading parameters. That implies that the flattening of the yield curve is captured by the slower convergence speed to the long-term level in the 2-factor model, while it is captured by the curvature factor in the 3-factor model. In addition, estimates of the time-varying specification follow a general downward trend over time.

To sum up the examinations of the estimated yield curve factors and the loading parameter, the following three points should be noted.

First, the level factors follow a general downward trend under the ultra-low interest rate environment in Japan. Furthermore, the estimates show somewhat volatile fluctuations, and this tendency is more pronounced in specifications with fixed loading parameter. Notably, they exhibit a significant drop following the introduction of the negative interest rate policy in 2016. This point requires caution when examining monetary policy indicators, as the effect of yield curve fluctuations depends heavily on the overall level of the yield curve.

Second, the flattening of the short-to-medium-term zone of the yield curve is captured as a steepening of the slope (an increase in the negative slope factor) by the 2-factor specification without the curvature factor. In contrast, it is detected by the 3-factor specification as a widening of the curvature (an increase in the negative curvature factor), indicating a significant downward dip in the yield curve.

Third, the overall flattening of the yield curve tends to be absorbed by a decline in the level factor in the fixed loading parameter estimation. It is captured by slower convergence to the long-term level in the time-varying loading parameter estimation.

4.3   Discussion on model selection

We examine additional issues in model selection for constructing monetary policy indicators from three perspectives: fixed or time-varying loading parameter; the height and stability of the level factor; and inclusion of a curvature factor.

The above estimation results show that the 3-factor model produces a higher estimation accuracy. In particular, for overall goodness-of-fit, SB-DNS-TVL(3), which allows the most flexible specification, performs best. However, B-AFNS(3) provides a better fit for the ultra-long-term zone. However, examining the trend of the estimated yield curve factors reveals that B-AFNS(3) exhibits high volatility in the level factor, which captures the long-term convergence level of the yield curve. That causes concern when constructing monetary policy indicators, as stable estimates of the long-term

level of the yield curve are expected.

4.3.1 Fixed versus time-varying loading parameter

The first issue is fixed or time-varying loading parameter. On this point, Shiratsuka (2025a) notes that the parameters of the nonlinear functional form, defined as the Nelson-Siegel model, are difficult to estimate robustly under the ultra-low interest rate environment in Japan. In particular, the estimates of the level and loading parameters are contaminated with each other, making it difficult to identify them precisely. To address this issue, allowing the loading parameters to vary over time is highly effective, without assuming the no-arbitrage condition.

To examine how estimates of the fixed loading parameter vary with changes in the estimation period, Figure 7 shows the results of estimating the loading parameters by shortening the end of the estimation period from December 2024 to March 2009 on a quarterly basis for B-AFNS in the upper panel and SB-DNS in the lower panel.

Figure 7: Robustness of Fixed Loading Parameter to Changes in Estimation Periods
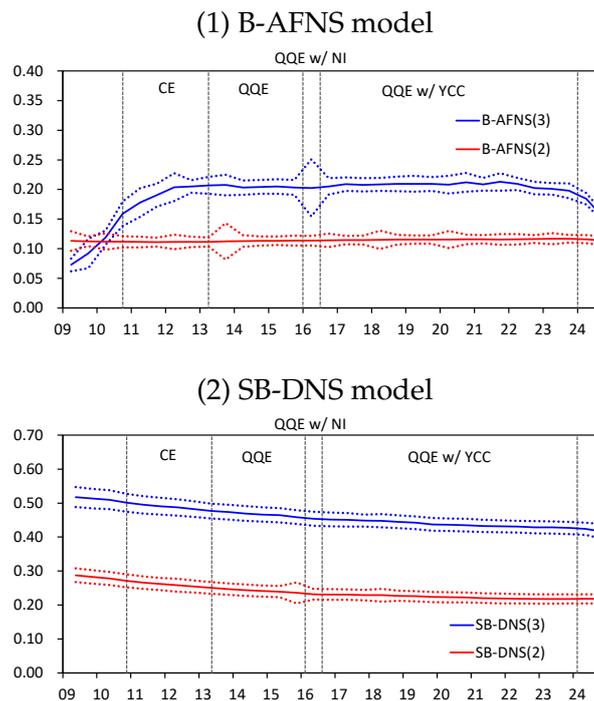
(1) B-AFNS model

(2) SB-DNS model

Notes: The plotted figures are estimates of the loading parameters by shortening the end of the estimation period from December 2024 to March 2009 on a quarterly basis. The bold and dotted lines indicate the estimates and their 2-standard-error confidence intervals, respectively. Regarding the abbreviations for the monetary policy regime, see the notes for Figure 1.

Looking first at the upper panel of the figure, B-AFNS(2) is largely unaffected by changes in the estimation period, while B-AFNS(3) is significantly affected. The esti-

mates for B-AFNS(3) increase until around 2012 as the estimation period is extended beyond 2009, then remain nearly constant before declining from around 2023.

Focusing on the confidence intervals, it is evident that for B-AFNS(3), the significant expansion during the introduction of the negative interest rate, coupled with a substantial overall decline and flattening of the yield curve, greatly impacted estimation accuracy. In contrast, while the intervals for B-AFNS(2) expanded slightly after the start of the QQE in 2013, they remained tight after the introduction of the negative interest rate, and no impact on estimation accuracy due to the negative interest rate policy can be confirmed. Furthermore, in the lower panel of the figure, SB-DNS(2) and (3) show a gradual downward trend. However, the confidence intervals remain narrow and the spread between the two remains stable.

It is thus deemed effective to allow the loading parameter to vary over time in precisely identifying the estimates of the level and loading parameters.

4.3.2 Height and stability of the level factor

The second issue is the height and stability of the level factor. Estimates with a time-varying loading parameter remain relatively stable at a high level, while estimates with a fixed loading parameter show a significant decline, as shown in Figure 6. Estimates with a fixed loading parameter may interpret the flattening of the yield curve as a decline in the overall level.

To examine the robustness of the level factor to changes in the estimation period, Figure 8 plots estimates of the level factor by reducing the end of the estimation periods from 2024 to 2010 for all six specifications. The figure shows that the estimates for B-AFNS(3) are significantly affected by changes in the estimation period. In particular, the deviations are prominent for the estimates of the estimation periods ending in 2010 and 2024, where the loading parameter is estimated at lower values than in other subsamples. In contrast, the estimates of other specifications remain largely unaffected.

4.3.3 Inclusion of curvature factor

The third issue is the effects of including or excluding the curvature factor, or the choice between the two- and 3-factor specifications.

Regarding the flattening of the short-to-medium-term zone of the yield curve, the 2-factor specification without the curvature factor captures it as a steepening of the slope (an increase in the negative slope factor). In contrast, a 3-factor specification with the curvature factor accounts for it as a widening of the curvature (an increase in the negative curvature factor), indicating a significant downward dip in the yield

25

Figure 8: Robustness of Level Factor to Changes in Estimation Periods
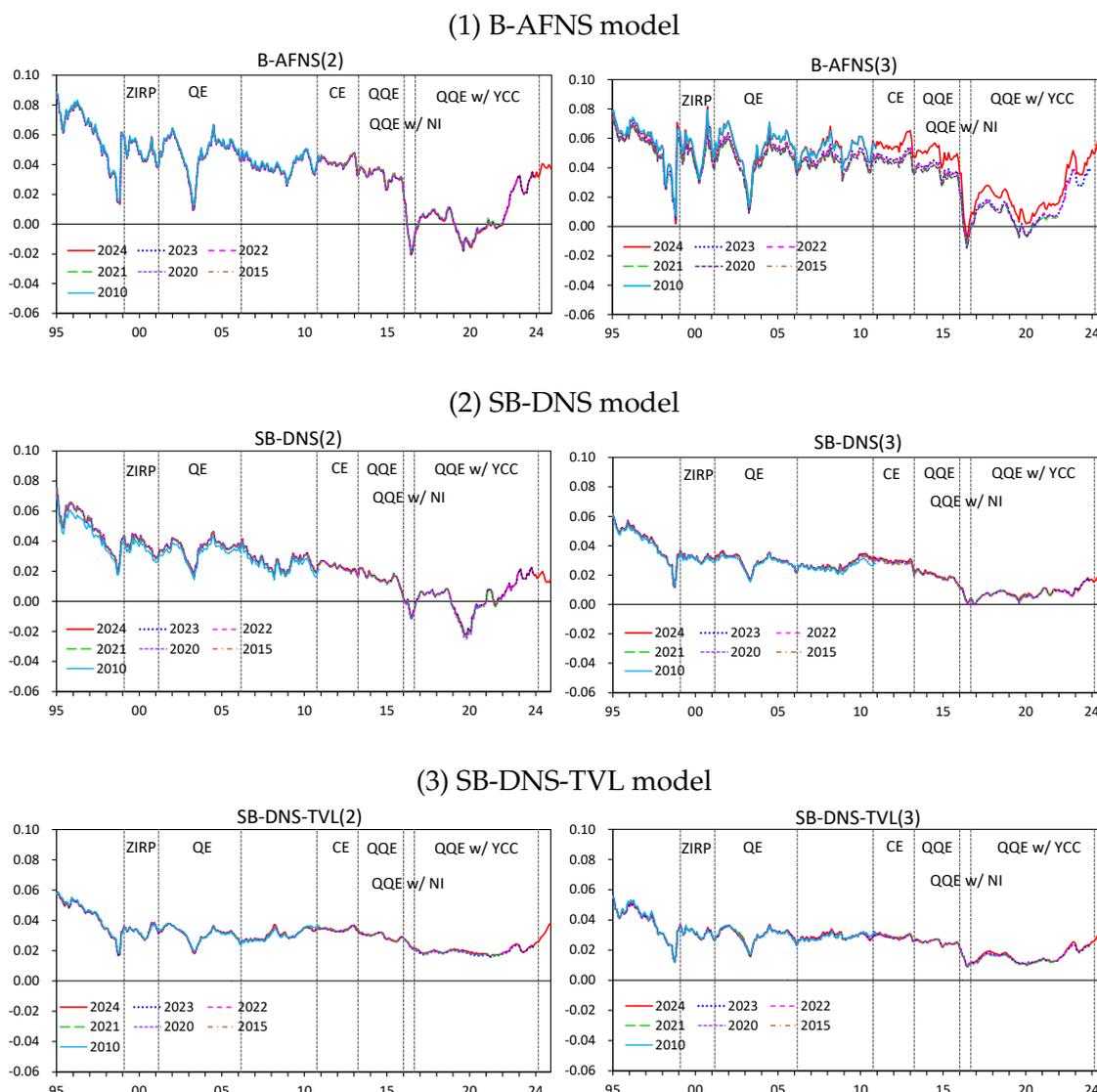
(1) B-AFNS model

(2) SB-DNS model


(3) SB-DNS-TVL model

Notes: The plotted figures are estimates of the loading parameters by shortening the end of the estimation period from end-2024 to end-2010. Regarding the abbreviations for the monetary policy regime, see the notes for Figure 1.

curve. Therefore, if unconventional monetary policy lowers the future path of the IFR in the short-to-medium-term zone of the yield curve, the 2-factor specification may interpret this as a larger downward shift of the short-end of the yield curve, suggesting a significant decline in the shadow interest rate.

Figure 9 shows scatter plots of the differences in the slope factor between the two- and 3-factor specifications on the vertical axis and the curvature factor for the 3-factor specification. The B-AFNS model in the left-hand panel of the figure clearly exhibits a shift in the relationship between the two variables, from downward-sloping to upward-

sloping around the time of the GFC. That indicates that, as the level of the yield curve declines, B-AFNS(3) captures the yield curve flattening as a more deeply dip-shape of the curvature factor, while B-AFNS(2) captures it as a steepening of the slope factor. In contrast, the SB-DNS model in the right-hand panel shows no clear relationship over time.

Figure 9: Relation between Slope and Curvature factors
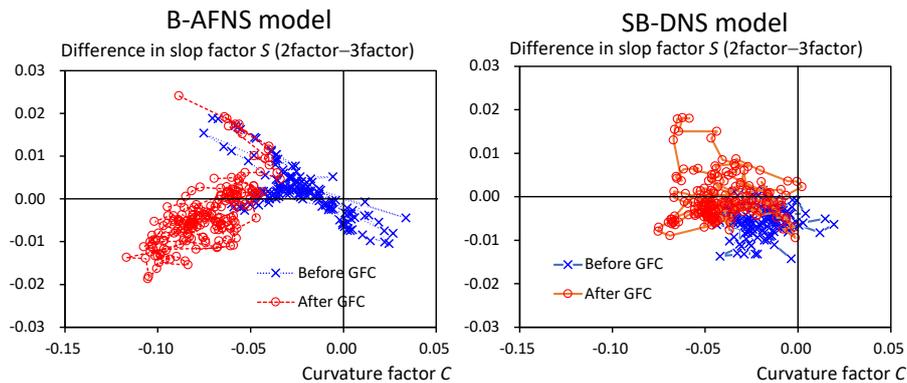
4.3.4　Model selection for monetary policy indicator construction

Based on the above examinations, we will examine monetary policy indicators in the next section by focusing on comparing three specifications — B-AFNS(2), B-AFNS(3), and SB-DNS-TVL(3) — selected from the six specifications estimated in this section.

B-AFNS(2) is the most widely used specification, assuming the no-arbitrage conditions and describing yield curve movements with two factors: level and slope. This specification serves as the benchmark for estimating the shadow interest rate. We compare this specification with B-AFNS(3), which describes yield curve fluctuations using three factors by additionally incorporating curvature, and SB-DNS-TVL(3), which maximizes the flexibility of the specification by not assuming the no-arbitrage condition and incorporating the time-varying loading parameter.

5　Monetary Policy Indicators

In this section, we construct monetary policy indicators based on the estimation results of SSR models. Given the discussion in the previous section, we focus on three of the six estimated shadow interest rate models: B-AFNS(2), B-AFNS(3), and SB-DNS-TVL(3).

It should be noted that the monetary policy indicators constructed below capture the expected effects of monetary policy, as reflected in the yield curve information.

Under the ELB constraint, monetary policy management relies heavily on expectations management. Therefore, we aim to examine how expectations regarding the future path of monetary policy in financial markets evolve in response to changes in economic and financial conditions.

5.1 Definition of monetary policy indicators

We construct three monetary policy indicators. In the following, we focus on the shape of the yield curve at a given time t to maturity τ. We denote the shadow IFR and the shadow spot rate, without assuming the lower bound constraint on the nominal interest rate, as $f_t(\tau)$ and $y_t(\tau)$, respectively. Here, the relationship with the future time T is given by $T = t + \tau$.

The first indicator is the shadow short-term rate (SSR), defined as the sum of a level and slope factors:

$$SSR_t = L_t + S_t = f_t(0) = y_t(0). \tag{30}$$

SSR corresponds to the shadow IFR at maturity zero and serves as an indicator of the policy interest rate in the absence of the lower bound on nominal interest rates. SSR is designed to address the problem that the monetary policy stance cannot be measured by the policy interest rate when monetary policy is constrained by the effective lower bound.

The second indicator is the long-term forward rate (LFR), which corresponds to the level factor.

$$LFR_t = L_t = f_t(\infty) = y_t(\infty). \tag{31}$$

LFR indicates the steady-state nominal interest rate level toward which the expected path of SSR converges in the long term. LFR is generally decomposed into the steady-state real interest rate, long-term inflation expectations, and the term premium. It is also the sum of the expected long-term level of the neutral interest rate and the term premium. Therefore, LFR is considered to reflect market expectations regarding long-term economic performance, such as growth rates and inflation rates.

The third indicator is the effective monetary stimulus (EMS), which captures the extent to which the forward rate curve is pushed downward from LFR over the period until maturity τ. $EMS(\tau)$ is calculated by dividing the integral value (area) of the gap between LFR and the shadow IFR over the period until maturity τ.

$$EMS(\tau) = \frac{1}{\tau} \int_{m=0}^{\tau} \{LFR_t - f_t(m)\}dm = LFR_t - y_t(\tau). \tag{32}$$

$EMS(0)$ equals the difference between LFR and SSR, since SSR represents the shadow spot interest rate at maturity zero.

Regarding EMS, we make the following two modifications to the original indicator by Krippner (2015). First, we include areas where the future path of the shadow interest rate is negative in the integration. Given that negative interest rate policy reduces the ELB constraint slightly into negative levels, we consider it necessary to capture the effects of downward pressure on the future path of the shadow IFR, including the negative interest rate region. Second, when constructing the indicator, we divided the area by maturity τ to express the effects of downward pressure in terms of the spot rate. This makes the quantitative meaning of the indicator clearer.

Furthermore, EMS is decomposed into the portion above the ELB ($KEMS(\tau)$) and the portion below the ELB (shadow EMS, $SEMS(\tau)$). $KEMS(\tau)$ is the indicator originally proposed by Krippner (2015), where the upper bound is the difference between the levels of LFR and the ELB. $SEMS(\tau)$ represents the potential downward pressure effect that is not actually observable due to the existence of the ELB constraint. The relationship between EMS, $KEMS$, and $SEMS$ is expressed mathematically as follows.

$$EMS_t(\tau) = KEMS_t(\tau) + SEMS_t(\tau), \tag{33}$$

$$KEMS_t(\tau) = \frac{1}{\tau} \int_{m=0}^{\tau} \{LFR_t - max[ELB_t, f_t(m)]\}dm, \tag{34}$$

$$SEMS_t(\tau) = -\frac{1}{\tau} \int_{m=0}^{\tau} min[0, f_t(m) - ELB_t]dm, \tag{35}$$

where ELB_t indicates the level of the ELB constraint at time t.

5.2 Monetary easing effects based on monetary policy indicators

We now compare monetary policy indicators computed from three shadow interest rate models: B-AFNS(2), B-AFNS(3), and SB-DNS-TVL(3). In the following, we examine SSR and EMS, focusing on both their absolute levels and their relative relationship to LFR.

5.2.1 Estimated monetary policy indicator (1): Shadow short-term interest rate

Focusing first on the SSR estimation results, Figure 10 plots the estimated SSR and LFR on the same diagram. As discussed earlier, it is critical to focus both on the absolute level and the relationship to *LFR* when evaluating the monetary policy indicators.

The three *SSR* estimates show qualitatively similar trends, significantly declining to negative territory with the introduction of unconventional monetary policy measures. After hitting the ELB in 1995, they dipped slightly negative with the ZIRP in 1999 and widened their negative level with the QE in 2001. Furthermore, it expanded the negative level during the CE in 2010 and the QQE in 2013, but remained largely flat after the QQE w/ NIR and QQE w/ YCC in 2016, and has been narrowing the negative level since around 2023.

Nevertheless, the three estimates show quantitatively different monetary easing effects. Overall, B-AFNS(2) shows a substantial decline into negative territory, while B-AFNS(3) shows a more limited decline. SB-DNS-TVL(3) exhibits a movement somewhere between the two. B-AFNS(2) particularly assesses the easing effect after introducing the QQE to a large extent, with the negative margin reaching around 4%. In contrast, B-AFNS(3) shows a smaller decline than during the QE period, and SB-DNS-TVL(3) is also roughly the same as during the QE period. However, the confidence intervals for B-AFNS(2) widen after the start of the QQE, suggesting that the estimates should be interpreted with caution. In this regard, those for B-AFNS(3) and SB-DNS-TVL(3) remain consistently tight, maintaining a sufficiently high level of estimation precision.

When evaluating the monetary easing effect by combining *SSR* with *LFR*, the results differ somewhat. In particular, immediately after the introduction of the negative interest rate policy in 2016, *LFR* estimates for B-AFNS(2) and (3) decline significantly, and the differences between *LFR* and *SSR* estimates become insignificant. In contrast, SB-DNS-TVL(3) generally produces stable *LFR* estimates, and fluctuations in their levels do not significantly affect the evaluation of *SSR*. Those results suggest that it is crucial to consider the relative relationship between *SSR* and *LFR* when evaluating *SSR* under the ultra-low interest rate environment in Japan.

### 5.2.2 Estimated monetary policy indicator (2): Effective monetary stimulus

We next examine the trend in *EMS*, which captures the monetary easing effect through the relationship between *LFR* and the forward rate curve, based on the shadow interest rate. Figure 11 plots *EMS* for maturities of 0-, 3-, 10-, and 30-year together with *LFR*. Note that, under the assumption of an ELB constraint on the nominal interest rate,

Figure 10: Monetary Policy Indicator (1):
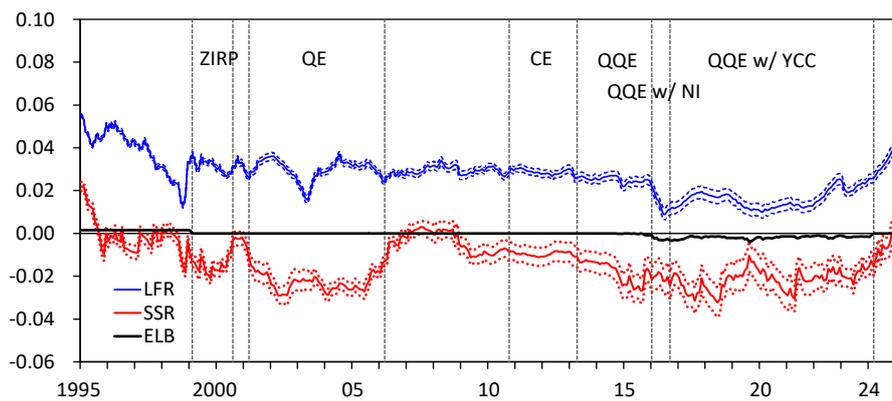## Shadow Short-term Interest Rate and Long-term Forward Rate

(1) B-AFNS(2)
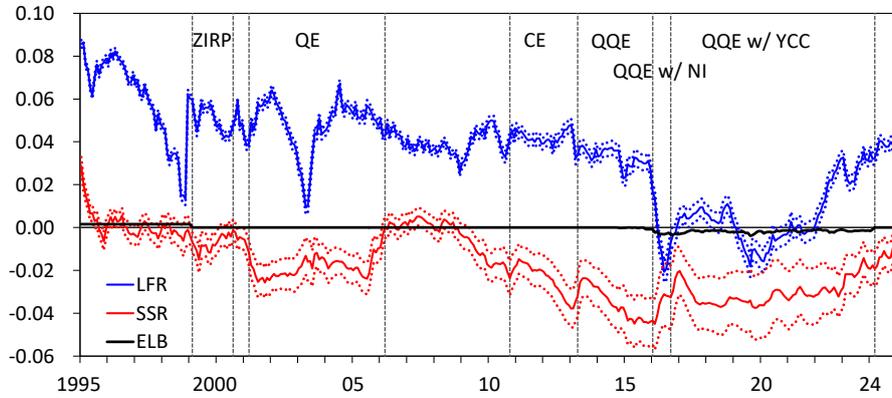
(2) B-AFNS(3)
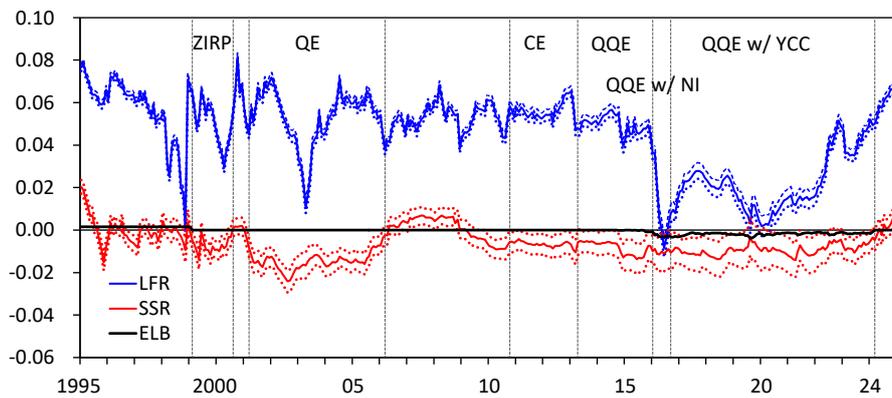
(3) SB-DNS-TVL(3)

Notes: The red and blue bold lines are SSR and LFR, respectively. The red and blue dotted lines indicate their 2-standard-error confidence intervals. Regarding the abbreviations for the monetary policy regime, see the notes for Figure 1.

SEMS (Equation (35)) is always zero, and *EMS* coincides with *KEMS*, with an upper bound equal to the difference between *LFR* and *ELB* (Equation (34)). However, in the shadow interest rate model without assuming the ELB constraint, *SEMS* takes a positive value, implying that *EMS* could exceed *LFR*.

B-AFNS(2) shows a generally high *EMS*, especially on short maturities of 0- and 3-year. In addition, *EMS*(10) for a 10-year maturity remains at a higher level than *LFR* since the start of the QQE in 2013, and *EMS*(30) for a 30-year maturity also exceeds *LFR* from 2016 to 2022 under the negative interest rate policy. These results imply that the monetary easing effect measured using B-AFNS(2) is driven by the portion of the estimated yield curve below the ELB constraint.

B-AFNS(3) generally exhibits movements similar to those of B-AFNS(2). However, *EMS*(0) and *EMS*(3) for maturities of zero and 3-year, respectively, are considerably smaller than those of B-AFNS(2), because the yield curve model incorporates a curvature term and the portion of the estimated yield curve below the ELB is smaller. Thus, the increase in EMS is limited during periods of significant yield curve declines under the negative interest rate policy implemented from 2016.

SB-DNS-TVL(3) stays at a lower level than B-AFNS(2) and B-AFNS(3), but it remains fairly stable over time. However, from 2016 to 2022, *EMS*(10) at 10-year maturity consistently exceeded *LFR*, thus indicating that monetary easing effects are driven by the portion of the estimated yield curve below the ELB constraint.

Figure 12 shows the decomposition results of *EMS*(30) for a 30-year maturity into *KEMS* and *SEMS*. Regardless of the specifications of the SSR models, qualitatively, *SMES* is observed only minimally during the QE period, expands after the GFC of 2008, and surges significantly immediately after the introduction of the negative interest rate policy in 2016 and during the COVID-19 turmoil of 2020. These observations confirm that the easing effects stemmed from lowering yield curve are mostly extracted from the yield curve below the ELB constraint after the introduction of the negative interest rate policy.

5.2.3   ELB constraint on monetary easing effects

In summary of the above estimation results, the evaluation of monetary easing effects, in terms of the degree of lowering the yield curve, is significantly influenced by the specification of the SSR models.

B-AFNS(2), which considers only the level and slope factors in yield curve dynamics, exhibits the largest easing effects, especially in relatively shorter-maturity zones. However, it is highly vulnerable to the significant and overall decline in the yield curve after the introduction of the negative interest rate policy in 2016. B-AFNS(3),

Figure 11: Monetary Policy Indicator (2):
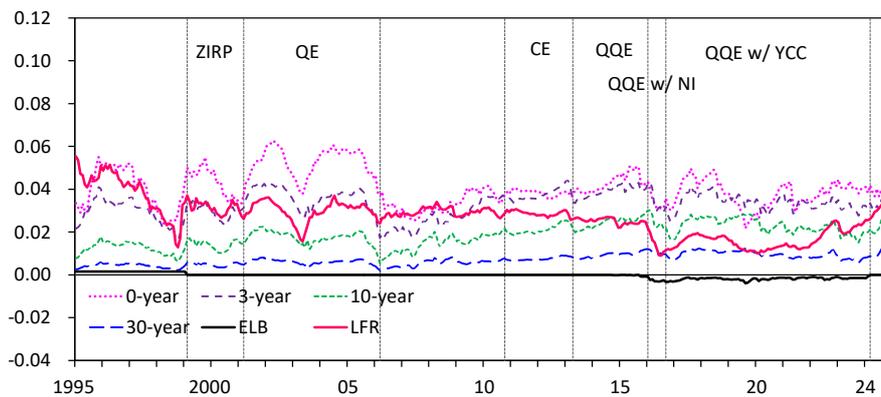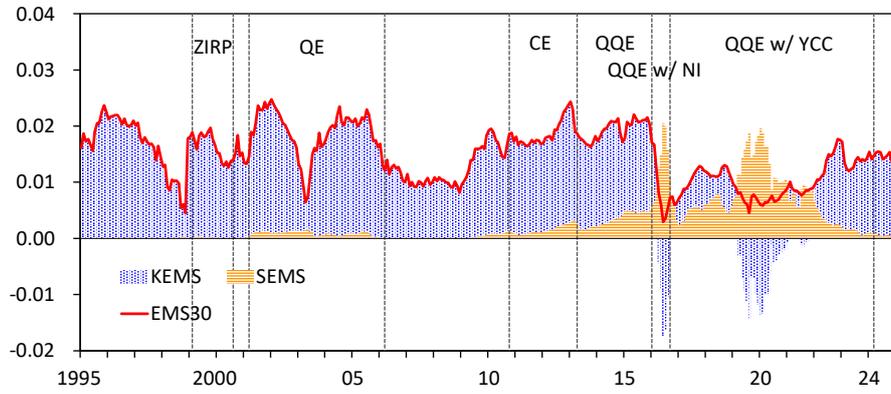Effective Monetary Stimulus

(1) B-AFNS(2)
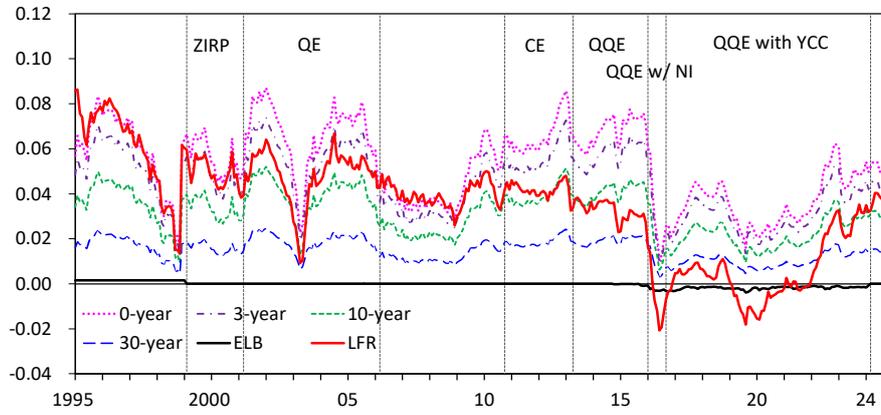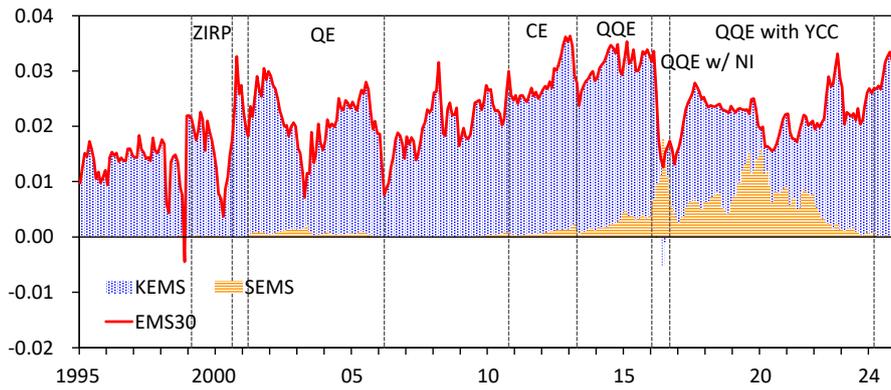
(2) B-AFNS(3)
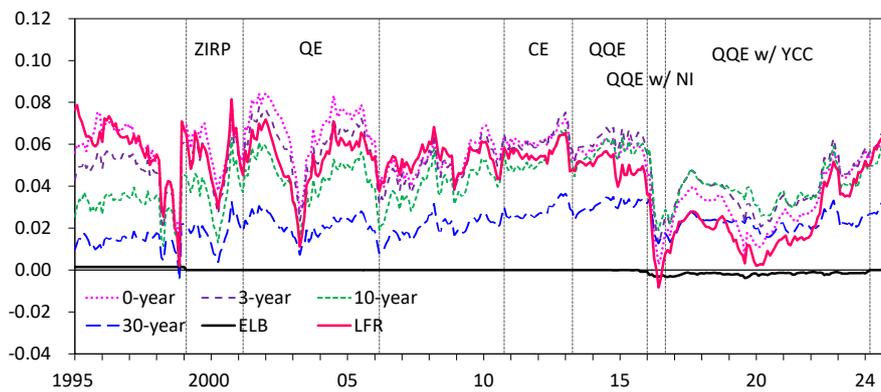
(3) SB-DNS-TVL(3)

Notes: Regarding the abbreviations for the monetary policy regime, see the notes for Figure 1.

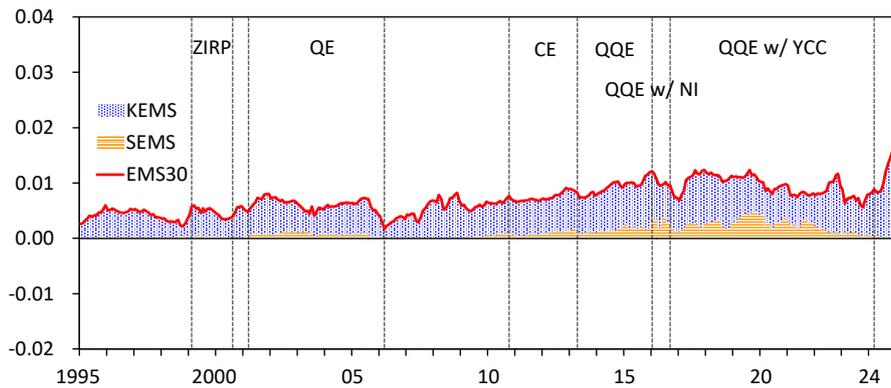# Figure 12: Decomposition of Effective Monetary Stimulus at 30-year Maturity

(1) B-AFNS(2)

(2) B-AFNS(3)

(3) SB-DNS-TVL(3)

Notes: Regarding the abbreviations for the monetary policy regime, see the notes for Figure 1.

which additionally considers the curvature factor, traces the easing effects from short-to medium-term maturities in a more balanced manner. However, it is also vulnerable to the significant and overall decline in the yield curve after 2016. SB-DNS-TVL(3), which makes the loading parameter time-varying, produces more stable easing effects, but generally estimates them somewhat smaller.

At the same time, however, the three SSR models show a common qualitative implication. Monetary policy did not produce significant easing effects, even with the introduction of a series of unconventional measures since the late 1990s. To explore this point further, we compare the SSR estimates with the Taylor rule, considering the ELB constraint on monetary easing effects.

The Taylor rule, proposed by Taylor (1993), is generally defined as:

$$i_t = r^* + \pi^* + \alpha(\pi_t - \pi^*) + \beta(y_t - y_t^*), \tag{36}$$

where i_t, r^*, π^*, π_t, y_t, and y_t^* are nominal policy interest rate in period t, the equilibrium real interest rate, the target inflation rate, the observed inflation rate in period t, the observed real GDP in period t, and the potential GDP in period t, respectively.

The inflation rate is the year-on-year change in the CPI (all items excluding fresh food and energy), adjusted for consumption tax. The output gap, or $y_t - y_t^*$, and the potential growth rate are estimates published by the Research and Statistics Department of the BOJ. The equilibrium real interest rate is assumed to equal the potential growth rate, converted from an original semi-annual basis to a quarterly basis using linear interpolation. For the Taylor rule parameters, following the original Taylor rule, we set $\alpha = 1.5$ and $\beta = 0.5$, with a target inflation rate of 2%.

Figure 13 plots the actual policy interest rate (uncollateralized overnight call rate), *SSR* for three specifications (B-AFNS(2), B-AFNS(3), and SB-DNS-TVL(3)), and the Taylor Rule. The monetary policy stance inferred from the shape of the yield curve (financial markets) is reflected in *SSR*, while the stance implied by macroeconomic variables is reflected in the Taylor Rule.

Looking at this figure, before the GFC of 2008, even while the policy interest rate was constrained by the ELB, the SSR and Taylor Rule declined to negative territory and generally followed very similar paths. During this period before 2008, the BOJ's unconventional monetary policy measures, such as the ZIRP and the QE, exerted an effective easing effect despite the ELB constraint on nominal interest rates.

The two indicators diverged significantly after the GFC of 2008. The Taylor rule remained responsive to fluctuations in macroeconomic conditions, especially huge adverse shocks, such as the GFC of 2008 and the COVID-19 turmoil of 2020. In contrast, although the SSR consistently remained in negative territory, even at different levels

Figure 13: *SSR* and Taylor rule
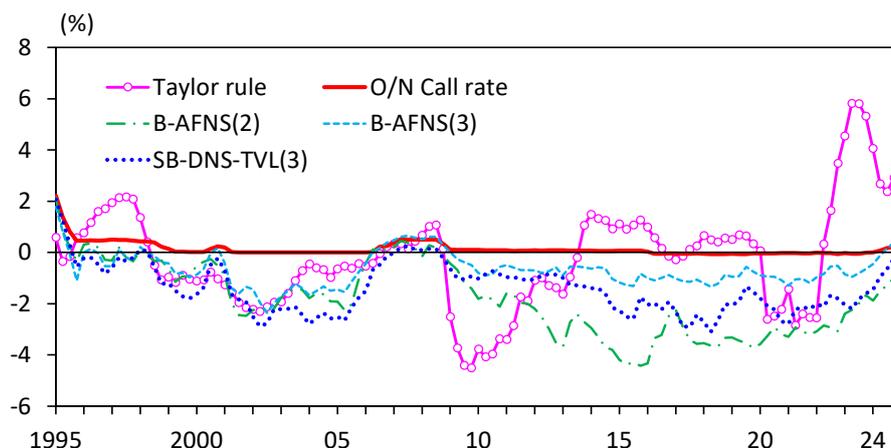
depending on the specifications, the SSR failed to respond to huge adverse shocks.

The above observations indicate that, under a prolonged period of ultra-low interest rate environment, it became increasingly difficult to adjust the monetary policy stance in response to changes in economic and financial conditions. Even with the SSR model, monetary policy was strongly constrained by the ELB on nominal interest rates.

In addition, such observations are consistent with the trend in *EMS* shown in Figure 11. Before the GFC of 2008, *EMS* for relatively short maturities, such as 0-year and 3-year, rose in response to new monetary easing measures, indicating that additional easing effects were being extracted. However, after the GFC, even with the introduction of the QQE, *EMS* reacted only moderately across maturities from short- to ultra-long-term.

6 Concluding Remarks

In this paper, we revisited shadow short-term interest rate (SSR) models using yield curve data from the prolonged ultra-low interest rate environment in Japan. By comparing various model specifications, we examined the trade-off between estimation performance and theoretical consistency in assessing monetary policy stances under the ELB constraint.

Our empirical analysis yielded three key findings. First, in terms of model specification, the choice between 2-factor and 3-factor models is a fundamental prerequisite. Although 2-factor models (level and slope only) are often preferred for their estimation stability, our findings demonstrate that a 3-factor model, which incorporates the

36

curvature factor, is essential in the Japanese context. Since the GFC of 2008, the curvature term has played an important role in capturing the downward pressure on the medium- to long-term zones of the yield curve. Building on this 3-factor structure, we further emphasize that allowing the loading parameter to vary over time is effective. This approach effectively addresses the contamination problem between the level and loading parameters, a significant challenge in fixed-parameter models under the ultra-low interest rate environment, thereby ensuring the precise identification and stability of the level factor, or the long-term forward rate (LFR).

Second, we highlighted the importance of evaluating monetary easing effects using information from the entire yield curve. In Japan's context, the shadow short-term interest rate (SSR) at zero maturity alone is insufficient to capture the comprehensive impact of unconventional monetary policy measures. Instead, the effective monetary stimulus (EMS), which reflects the downward pressure across the yield curve, provides a more appropriate picture of the policy stance. These observations confirm the importance of examining market expectations for the future path of monetary policy when evaluating monetary policy effects in the ultra-low interest rate environment.

Third and finally, we showed that the comparison between SSR and the Taylor rule revealed that the easing effects of unconventional monetary policy measures have been strongly restricted by the effective lower bound (ELB) constraint since the GFC of 2008. Although the Bank of Japan (BOJ) implemented large-scale unconventional monetary policy measures, the downward shift of the entire yield curve limited the room for further stimulus. These findings suggest that for central banks facing the ELB, monitoring a suite of indicators, including SSR, LFR, and EMS, is highly effective in assessing monetary policy under the prolonged ultra-low interest rate environment in Japan.

As a direction for future research, it would be highly valuable to estimate vector autoregression (VAR) models that incorporate the indicators developed in this paper, such as SSR and EMS, as policy variables. Such an approach would enable a more comprehensive analysis of the macroeconomic impacts of unconventional monetary policy under the ELB constraint. In conducting such analyses, it is essential to emphasize the perspective established in this paper: evaluating the monetary policy stance by combining SSR with LFR. By accounting for the long-term convergence level of interest rates alongside the shadow short-term rate, the effectiveness of unconventional monetary policy in an ultra-low interest rate environment is able to be more accurately captured.

References

Black, F., 1995. Interest rates as options. The Journal of Finance 50, 1371–1376. doi:https://doi.org/10.1111/j.1540-6261.1995.tb05182.x.

Christensen, J.H.E., Diebold, F.X., Rudebusch, G.D., 2011. The Affine Arbitrage-free Class of Nelson-Siegel Term Structure Models. Journal of Econometrics 164, 4–20. doi:10.1016/j.jeconom.2011.02.011.

Christensen, J.H.E., Rudebusch, G., 2015. Estimating Shadow-Rate Term Structure Models with Near-Zero Yields. Journal of Financial Econometrics 13, 226–259.

Christensen, J.H.E., Rudebusch, G.D., 2019. A new normal for interest rates? evidence from inflation-indexed debt. The Review of Economics and Statistics 101, 933–949. doi:10.1162/rest_a_00821.

van Dijk, D., Koopman, S.J., van der Wel, M., Wright, J.H., 2014. Forecasting Interest Rates with Shifting Endpoints. Journal of Applied Econometrics 29, 693–712. doi:10.1002/jae.2358.

Duffee, G.R., 2002. Term premia and interest rate forecasts in affine models. The Journal of Finance 57, 405–443. doi:https://doi.org/10.1111/1540-6261.00426.

Fisher, M., Gilles, C., 1996. Term premia in exponential-affine models of the term structure. Mimeo, The Board of Governors of the Fedearl Reserve System.

Fujiki, H., Shiratsuka, S., 2002. Policy Duration Effect under the Zero Interest Rate Policy in 1999-2000: Evidence from Japan's Money Market Data. Monetary and Economic Studies 20, 1–31.

Ichiue, H., Ueno, Y., 2013. Term premia in exponential-affine models of the term structure. Technical Report 13-E-8. Bank of Japan.

Kim, D.H., Priebsch, M.A., 2024. Are shadow rate models of the treasury yield curve structurally stable? Journal of Financial and Quantitative Analysis 59, 3500–3530. doi:10.1017/S0022109023000984.

Kim, D.H., Singleton, K.J., 2012. Term structure models and the zero bound: An empirical investigation of japanese yields. Journal of Econometrics 170, 32–49. doi:https://doi.org/10.1016/j.jeconom.2011.12.005.

Koeda, J., Sekine, A., 2022. Nelson-Segel decay factor and term premia in Japan. Journal of the Japanese and International Economies 64, 101204. doi:https://doi.org/10.1016/j.jjie.2022.101204.

Kortela, T., 2016. A shadow rate model with time-varying lower bound of interest rates. Bank of Finland Research Discussion Papers 19/2016. Bank of Finland. doi:None.

Krippner, L., 2012. Modifying Gaussian Term Structure Models When Interest Rates are Near the Zero Lower Bound. Technical Report. Reserve Bank of New Zealand. doi:10.2139/ssrn.1950439.

Krippner, L., 2015. Zero Lower Bound Term Structure Modeling: A Practitioner's Guide. Palgrave Macmillan.

Krippner, L., 2020. A note of caution on shadow rate estimates. Journal of Money, Credit and Banking 52, 951–962. doi:https://doi.org/10.1111/jmcb.12613.

Nelson, C.R., Siegel, A.F., 1987. Parsimonious Modeling of Yield Curves. The Journal of Business 60, 473–489. doi:10.1086/296409.

Okina, K., Shiratsuka, S., 2004. Policy Commitment and Expectation Formation: Japan's Experience under Zero Interest Rates. The North American Journal of Economics and Finance 15, 75–100. doi:10.1016/j.najef.2003.11.001.

Opschoor, D., van der Wel, M., 2022. A Smooth Shadow-Rate Dynamic Nelson-Siegel Model for Yields at the Zero Lower Bound. Technical Report 22-011. Tinbergen Institute.

Opschoor, D., van der Wel, M., 2025. A smooth shadow-rate dynamic nelson-siegel model for yields at the zero lower bound. Journal of Business and Economic Statistics 43, 298–311. doi:10.1080/07350015.2024.2365779.

Shiratsuka, S., 2025a. Monetary policy effectiveness under the ultra-low interest rate environment: Evidence from yield curve dynamics in japan. Oxford Bulletin of Economics and Statistics 87, 98–121. doi:https://doi.org/10.1111/obes.12635.

Shiratsuka, S., 2025b. What did the bank of japan do under the yield curve control policy? Journal of the Japanese and International Economies 76, 101352. doi:https://doi.org/10.1016/j.jjie.2025.101352.

Swanson, E.T., Williams, J.C., 2014. Measuring the effect of the zero lower bound on medium- and longer-term interest rates. American Economic Review 104, 3154–85. doi:10.1257/aer.104.10.3154.

Taylor, J.B., 1993. Discretion versus policy rules in practice. Carnegie-Rochester Conference Series on Public Policy 39, 195–214. doi:https://doi.org/10.1016/0167-2231(93)90009-L.

Wu, J.C., Xia, F.D., 2016. Measuring the Macroeconomic Impact of Monetary Policy at the Zero Lower Bound. Journal of Money, Credit and Banking 48, 253–291. doi:10.1111/jmcb.12300.